Stony Brook University

Negative charges at Mek1 kinase consensus sites downregulate Ndt80 activity during budding yeast meiotic prophase without affecting protein stability

A Thesis Presented

by

Robert Gaglione

to

The Graduate School

in Partial Fulfillment of the

Requirements

for the Degree of

Master of Science

in

Biochemistry and Cell Biology

Stony Brook University

December 2017

Stony Brook University

The Graduate School

Robert Gaglione

We, the thesis committee for the above candidate for the

Master of Science degree, hereby recommend

acceptance of this thesis.

Nancy M. Hollingsworth – Thesis Advisor
SUNY Distinguished Teaching Professor
Department of Biochemistry and Cell Biology

Bruce Futcher – Second Reader
Professor
Department of Molecular Genetics and Microbiology

This thesis is accepted by the Graduate School

Charles Taber
Dean of the Graduate School

Abstract of the Thesis

Negative charges at Mek1 kinase consensus sites downregulate Ndt80 activity during budding yeast meiotic prophase without affecting protein stability

by

Robert Gaglione

Master of Science

in

Biochemistry and Cell Biology

Stony Brook University

2017

Meiotic recombination promotes the formation of crossovers between homologous chromosomes to ensure their proper segregation in Meiosis I. Crossovers are formed by the repair of programmed double strand breaks (DSBs) during meiotic prophase. In budding yeast, the meiotic recombination checkpoint delays meiotic progression until all DSBs have been repaired and is under the control of the meiosis-specific Mek1 kinase. The meiosis-specific transcription factor Ndt80 activates the transcription of hundreds of genes, including those required for prophase exit and the meiotic divisions. Transcription of *NDT80* occurs in two stages, mediated first by Ime1 and then by Ndt80 itself. Ime1-transcribed Ndt80 is negatively regulated by the checkpoint, preventing the expression of *NDT80* and its downstream targets. Mutated strains which arrest due to unresolved DSBs accumulate inactive Ndt80 in the cytoplasm. Ndt80 contains six putative Mek1 consensus sequences within its DNA-binding domain. While preventing phosphorylation at these sites using alanine substitutions (*ndt80-6A*) does not affect Ndt80 activity, aspartic acid substitutions (*ndt80-6D*), which may mimic the negative charge of phosphorylation, make Ndt80 constitutively inactive. Immunoblot analyses showed that *ndt80-6D* prevents

accumulation of Ndt80-dependent gene products, including Ndt80 itself. When the *NDT80* gene was put under the control of an inducible promoter, Ndt80-6D protein levels were equivalent to wild-type, although no downstream targets were detected. This result shows that negative charges do not affect Ndt80 protein stability, but instead prevent the accumulation in Ndt80 protein that results from Ndt80-mediated transcription of *NDT80*. In addition, a fluorescence-based system was developed to allow for the visualization of Ndt80 localization in live cells.

Table of Contents

List of Figures and Tables

List of Abbreviations

amp: ampicillin

ATP: adenosine triphosphate

bp: basepair

°C: degrees Celsius

CDK: cyclin-dependent kinase

DAPI: 4',6-diamidino-2-phenylindole

DBD: DNA-binding domain

DDK: Dbf4-dependent kinase (Cdc7-Dbf4)

DIC: differential interference contrast

dH_2O: deionized water

dNTP: deoxynucleotide triphosphate

DNA: deoxyribonucleic acid

DSB: double-stranded break

E. coli: *Escherichia coli*

ED: β-estradiol

EDTA: Ethylenediaminetetraacetic acid

FITC: fluorescein isothiocyanate

5-FOA: 5-fluoroorotic acid

G418: geneticin

GAL4-ER: *GAL4*-mammalian estrogen receptor fusion

GFP: green fluorescent protein

HygB: hygromycin

I: 1-NA-PP1 (see 1-NA-PP1)

Kb: kilobase

L: liter

LB: lysogeny broth

M: molar

MI: Meiosis I

MII: Meiosis II

µL: microliter

mL: milliliter

µM: micromolar

mM: millimolar

MSE: middle sporulation element

1-NA-PP1: 1-(1,1-dimethylethyl)-3-(1-napthalenyl)-1H-pyrazolo[3,4-d]pyrimidin-4-amine

NAT: nourseothricin

NDT80-6A: *NDT80- S24A S205A T211A S327A S329 S343A*

NDT80-6D: *NDT80- S24D S205D T211D S327D S329D S343D*

NDT80-IN: inducible *NDT80*

ng: nanogram

nm: nanometer

ORF: open reading frame

P_{GAL1}: Promoter of *GAL1*

PCR: polymerase chain reaction

PVDF: polyvinylidine difluoride

RPM: revolutions per minute

SC: synaptonemal complex

SD: synthetic defined

SDS: sodium dodecylsulfate

SOC: super optimal broth with catabolite repression

Spo: Sporulation medium

TCA: trichloroacetic acid

TAE: Tris base – acetic acid - EDTA

TBE: Tris base – boric acid – EDTA

TE: 10 mM Tris-HCl, pH 8.0 and EDTA

UTR: untranslated region

WT: wild type

YPA: yeast extract peptone acetate

YPD: yeast extract peptone dextrose

Acknowledgements

I would like to thank Nancy M. Hollingsworth for her guidance, patience, and support throughout the successes and challenges surrounding my project. Through her amazing mentorship, I have learned not only the techniques used by a yeast genetics lab but also the challenging yet rewarding nature of academic research. I would also like to thank the members of the Hollingsworth lab, especially Xiangyu Chen, Cameron Burnett, Lihong Wan, and Dimitri Joseph for their patient assistance throughout my time in the lab. In addition to the members of the Hollingsworth lab, I would like to thank Ed Luk and the members of his lab for insightful scientific discussion. Many thanks to Aaron Neiman, Jae-Sook Park, and Reuben Hoffman for graciously letting me use their fluorescence microscope and for their assistance with the live imaging. Thank you to Neta Dean for her support and guidance throughout my time in the Biochemistry and Cell Biology Master of Science program and for letting me use her fluorescent microscope. Thank you to Bruce Futcher for being my second reader for this thesis. Thank you to Gang Zhao for providing the pFA6a-kanMX6-3xGFP plasmid and to Yuping Chen for providing the pRS425-GAL1-sc5xGFP11 and pRS425-TEF1-GFP1-10-IDT plasmids.

Introduction

Sexually reproducing organisms use the specialized meiotic cell division to produce haploid daughter cells from a diploid parental cell. Unlike mitosis, where cells undergo a single round of deoxyribonucleic acid (DNA) replication followed by an equational division of identical sister chromatids into daughter cells, meiosis involves a unique reductional division, where homologous pairs of chromosomes separate prior to an equational division. The meiotic program is also characterized by the exchange of genetic information caused by homologous recombination. This process physically links homologous chromosomes, allowing for their proper alignment at the metaphase plate and segregation to opposite spindle poles during Anaphase I. Errors in this process can lead to nondisjunction, where homologs fail to correctly segregate, and ultimately the formation of aneuploid daughter cells. In addition to being the leading genetic cause of miscarriages, human aneuploidies result in genetic disorders, including Down and Kleinfelter syndromes (Hassold and Hunt, 2001). The critical importance of meiosis for eukaryotic reproduction is evidenced by its evolutionarily conservation. This conservation makes the budding yeast, *Saccharomyces cerevisiae*, an excellent model system to decipher the molecular and genetic processes required to faithfully segregate chromosomes (Loidl, 2016).

Recombination begins with the introduction of DNA double-stranded breaks (DSBs) throughout the genome (Sun et al., 1989), catalyzed by the topoisomerase-like protein Spo11 (Bergerat et al., 1997; Cao et al., 1990; Keeney et al., 1997). 5’ to 3’ exonucleolytic digestion of the breaks results in 3’ overhangs on each side (Sun et al., 1991), allowing the RecA homologs Dmc1 and Rad51 to form complexes on the 3’

single strand ends (Bishop, 1994; Brown et al., 2015). The nucleoprotein filaments enable the activity of the meiosis-specific Dmc1 to search for a homologous chromatid to mediate invasion of the 3' single strand end (Cloud et al., 2012; Dresser et al., 1997; Hong et al., 2001). Strand invasion intermediates are then processed either to form crossovers or non-crossovers using several different pathways (Kohl and Sekelsky, 2013).

Homolog synapsis occurs by the formation of a protein-based homolog-pairing structure known as the synaptonemal complex (SC) (Padmore et al., 1991). Axial elements are first formed by condensation of sister chromatids along protein cores comprised of the meiosis-specific proteins Hop1, Red1, and Rec8 (Hollingsworth et al., 1990; Klein et al., 1999; Smith and Roeder, 1997). Homologous axial elements are then brought together by the processing of strand invasion intermediates using a group of functionally diverse proteins collectively encoded by the "ZMM" pathway (Börner et al., 2004; Lynn et al., 2007). Synapsis occurs when the transverse filament protein, Zip1, assembles along the lengths of the axial elements, holding the two homologs together (Dong and Roeder, 2000; Sym et al., 1993; Tung and Roeder, 1998). The ZMM pathway is required not only for synapsis, but also for creating recombination intermediates that are resolved solely as crossovers. These crossovers, in combination with sister chromatid cohesion, physically link homologs during meiotic prophase, promoting correct Meiosis I disjunction.

The formation of DSBs initiates a series of regulatory events, the meiotic recombination or pachytene checkpoint, that delay meiotic progression until the breaks have been repaired (Lydall et al., 1996). DSBs activate the Mec1 and Tel1 DNA-

damage response kinases to phosphorylate Hop1 (Carballo et al., 2008). The meiosis-specific checkpoint kinase, Mek1, is then recruited to the axial elements through its Forkhead-associated domain, which binds to phosphorylated Hop1, allowing for activation by *trans*-autophosphorylation (Carballo et al., 2008; Niu et al., 2007; Rockmill and Roeder, 1991; Wan et al., 2004). Dmc1-dependent interhomolog strand invasion is favored over that of Rad51 in meiotic cells due to the Mek1-mediated suppression of Rad51 activity by targeting its association with Rad54 (Callender et al., 2016; Liu et al., 2014; Niu et al., 2005). Mek1 also influences the resolution of synapsed chromosomes through the Cdc7-Dbf4 (DDK) kinase-mediated phosphorylation of Zip1, which promotes crossover formation through the action of the Zmm proteins (Chen et al., 2015). Mek1 activity ensures that DSBs are repaired before the first meiotic division by preventing progression past prophase (Xu et al., 1997). In *dmc1*Δ mutants, the continued suppression of Rad51-mediated strand invasion leaves unrepaired breaks, leading to a prophase arrest state that prevents sporulation (Bishop et al., 1992; Callender et al., 2016; Niu et al., 2009; Xu et al., 1997).

Ndt80 is a meiosis-specific transcription factor involved in the activation of hundreds of genes required for the meiotic divisions and sporulation (Chu et al., 1998; Chu and Herskowitz, 1998; Xu et al., 1995). Transcription of *NDT80* is initiated by the Ime1 transcription factor (Chu and Herskowitz, 1998; Pak and Segall, 2002). Ime1-mediated expression first requires inactivation of the Sum1-Rfm1-Hst1 transcriptional repressor complex due to Ime2-, cyclin-dependent kinase (CDK)-, and DDK-mediated phosphorylation of Sum1 (Ahmed et al., 2009; Benjamin et al., 2003; Lo et al., 2012; Shin et al., 2010; Winter, 2012). Since *IME2* transcription depends on Ime1, there is a

delay in the transcription of *NDT80* relative to other Ime1-dependent genes such as *SPO11*, *HOP1*, and *MEK1* (Pak and Segall, 2002). Transcriptional activity of the Ndt80 protein generated by Ime1 is activated by IME2-dependent phosphorylation and repressed by Mek1 (Benjamin et al., 2003; Pak and Segall, 2002; Sopko et al., 2002; Xu et al., 1997).

The primary sequence of Ndt80 can be divided into three segments, an N-terminal DNA binding domain (DBD), a “middle region” required for checkpoint inactivation and a C-terminal activation domain (Lamoureux et al., 2002; Sopko et al., 2002; Wang et al., 2011) (Fig 1-1A). Ndt80 is a site-specific DNA binding protein that recognizes a 9 basepair (bp) sequence called the middle sporulation element (MSE) present in the promoters of its targets, the middle sporulation genes (Chu and Herskowitz, 1998; Hepworth et al., 1995; Ozsarac et al., 1997). Genes transcribed by Ndt80 during meioisis include *CDC5*, involved in crossover resolution and SC disassembly, and *CLB1*, which allows for progression into Meiosis I (Carlile and Amon, 2008; Chu and Herskowitz, 1998; Dahmann and Futcher, 1995; Sopko et al., 2002; Sourirajan and Lichten, 2008). Ndt80 also binds to MSEs in its own promoter, creating an autoregulated amplification of the *NDT80* gene product and increased expression of downstream targets, allowing for prophase exit (Chu and Herskowitz, 1998).

In *dmc1*Δ checkpoint-arrested cells, reduced quantities of Ndt80 are observed and its target genes are not expressed (Chu and Herskowitz, 1998; Hepworth et al., 1998). Ndt80 is directly regulated by the checkpoint, in part through the loss of activating phosphorylation of Ndt80 (Tung et al., 2000). In the BR genetic background, *zip1*Δ mutants arrest in prophase with connected but unsynapsed homologs (Sym et al.,

1993). In these cells, Ndt80 protein is localized primarily to the cytoplasm, preventing its activity as a transcription factor (Storlazzi et al., 1996; Sym et al., 1993; Wang et al., 2011). In contrast, *NDT80* mutants with an in-frame internal deletion of residues 346-402 (Figure 1-1A), labeled the bc region, are localized to the nucleus and *ndt80-bc zip1*Δ strains do not arrest. The "bc" domain is located in the middle region, between the N-terminal DNA binding domain and the C terminal activation domain (Figure 1-1A).

MEK1 is required for the meiotic recombination checkpoint (Wan et al., 2004; Xu et al., 1997). A fragment of Ndt80 containing the middle region and the activation domain were identified in a two-hybrid screen using lexA-Mek1 as bait (N. M. Hollingsworth, personal communication). These results suggest that Mek1 may delay/arrest cells in response to DSBs by directly phosphorylating Ndt80. In fact, the primary sequence of the Ndt80 protein contains 10 Mek1 substrate consensus sequences, RXXT/S (Mok et al., 2010; Suhandynata et al., 2016) (Figure 1-1A). In addition, phosphorylation of two amino acids in non-consensus sites within the middle region has been observed *in vivo* from a mass spectrometry-based phosphoproteomic analysis (Figure 1-1A) (Suhandynata et al., 2016). Mutation of the eight Mek1 consensus sites in the DBD and middle region as well as the two mass spectrometry sites allowed 31% sporulation in the *dmc1*Δ background, compared to 1.1% in *NDT80 dmc1*Δ, supporting the hypothesis that phosphorylation of these sites is important for checkpoint arrest (X. Chen and N. M. Hollingsworth, unpublished data). In contrast, substituting these 10 amino acids with aspartic acid, a negatively charged amino acid that can sometimes mimic phosphorylation, greatly reduced sporulation in both *dmc1*Δ and *DMC1* diploids (X. Chen and N. M. Hollingsworth, unpublished data). Furthermore,

aspartic acid substitutions of the Mek1 consensus sites in the DBD (S24D S205D T211D S327D S329D S343D, *ndt80-6D*) were sufficient to make Ndt80 constitutively inactive. These results suggest that the meiotic recombination checkpoint acts through Mek1 phosphorylation of DBD residues to inhibit Ndt80.

At least four of the putative substrates in the DBD are located on the DNA-protein interface, suggesting that their phosphorylation could repulse the negatively charged DNA and prevent Ndt80 activity (Figure 1-1B) (Lamoureux and Glover, 2006). In addition, an *in vitro* kinase assay has demonstrated that at least one of the DBD consensus sites is directly phosphorylated by Mek1 (X. Chen, unpublished data). One goal of my thesis was to use immunoblot analysis of Ndt80 DBD mutants and the accumulation patterns of their gene products to analyze the roles of the putative DBD substrates in Ndt80 regulation. In addition, I developed a system to fluorescently monitor Ndt80 in live cells to assist future efforts to characterize its regulation through cytoplasmic localization.

`

A

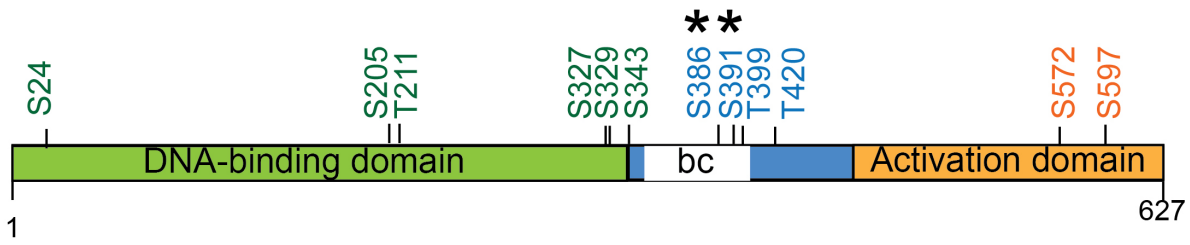

B

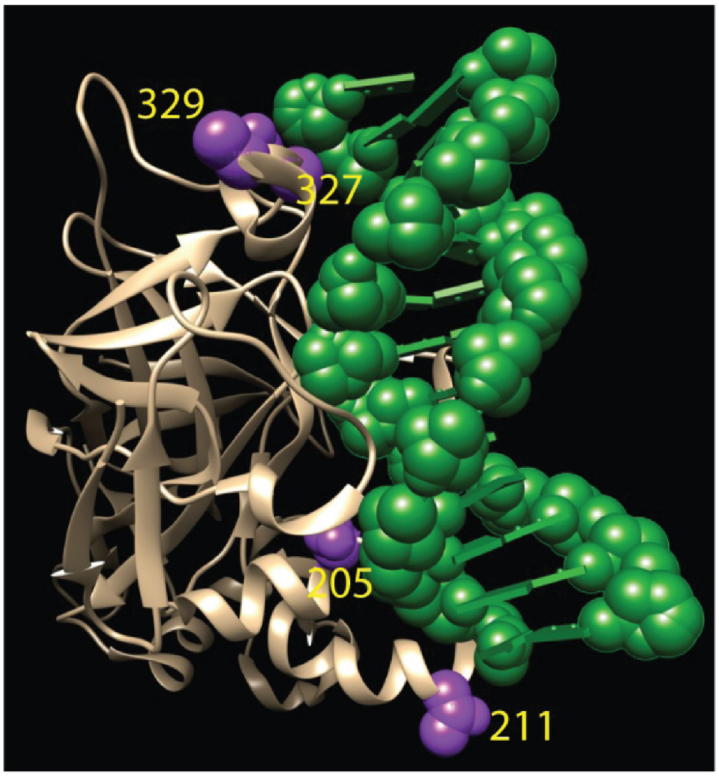

Figure 1-1. **Location of putative Mek1 consensus sites on Ndt80** (A) Different domains of Ndt80 are represented with locations of putative Mek1 substrates annotated. The middle region is indicated in blue. “bc” indicates a 60 amino acid domain required for checkpoint inactivation of Ndt80 (Wang et al., 2011). Residues with asterisks were phosphorylated in a *MEK1*-dependent manner in a phosphoproteomic analysis (Suhandynata et al., 2016). (B) Crystal structure of Ndt80 DNA-binding domain associated with an MSE sequence. Four potential Mek1 phosphosites in the DBD are shown as purple space-filling models. The MSE DNA is shown as a green space-filling model. Adapted by N. M. Hollingsworth from (Lamoureux and Glover, 2006).

Results

Constitutive negative charges on the Ndt80 DNA binding domain prevent accumulation of Ndt80 and other middle gene proteins

The observation that the *ndt80-6D* mutant fails to sporulate is consistent with the hypothesis that the negative charges conferred by aspartate are mimicking phosphorylation, resulting in constitutive inactivation of the transcription factor. However, *NDT80* is required for transcription of numerous genes, including those necessary for spore formation (Chu et al., 1998), so a specific downstream defect in spore formation cannot be ruled out. To determine whether *ndt80-6D* is defective in the transcription of targets required for the completion of recombination and meiotic progression (i.e., *CDC5* and *CLB1)*, meiotic timecourse analysis was carried out using liquid cultures of strains expressing *NDT80, ndt80-6A, ndt80-6D,* and *ndt80-R177A*. The R177A mutation substitutes a conserved arginine residue required for DNA binding with alanine and serves as a negative control (Montano et al., 2002).

After the cells were transferred to liquid sporulation (Spo) medium to induce meiosis, samples were taken at various timepoints, fixed with formaldehyde and the nuclei were visualized using the fluorescent dye, 4',6-diamidino-2-phenylindole (DAPI). Cells that have undergone Meiosis I or Meiosis II contain two or four nuclei, respectively. The *NDT80* and *ndt80-6A* strains progressed through the meiotic divisions at similar rates while the *ndt80-6D* and *ndt80-R177A* strains showed no progression over the first 12 hours in Spo medium (Figure 2-1B). Twenty-four hours after transfer to Spo medium, the *ndt80-6A* strain had slightly higher sporulation than wild type (WT) (92% compared to 88%), while neither the *ndt80-6D* nor the *ndt80-R177A* diploids

formed spores, consistent with sporulation results obtained using solid Spo medium (X. Chen, unpublished data).

Ndt80 transcriptional activity was monitored indirectly by looking at the protein products of Ndt80 targets, *NDT80*, *CDC5* and *CLB1*. In the *NDT80* strain, Ndt80, Cdc5, and Clb1 were observed after 4 hours in Spo medium and the levels of all three proteins decreased by 8 hours (Figure 2-1A and C). A similar pattern was observed for *ndt80-6A*, with the timing of the appearance of Cdc5 and Clb1 correlating with peak levels of Ndt80-6A (Figure 2-1A and C). The levels of Ndt80-6A, Cdc5 and Clb1 were reduced by 8 hours, with further reduction observed by 10 hours. The loss of certain protein samples from these strains prevents comparisons between the 4 and 6 hour timepoints, but after 8 and 10 hours, the *ndt80-6A* strain appeared to produce more Ndt80-6A, Cdc5, and Clb1 protein compared to WT. This could involve the loss of negative Ndt80 regulation in the 6A mutant, allowing it to enhance the expression of itself and middle genes before WT Ndt80, which would be negatively regulated by the checkpoint. Ndt80-6D was seen at 4 hours and slowly accumulated throughout the timecourse but even by 10 hours had not reached the peak level of WT protein (Figure 2-1A and C). This pattern of protein accumulation was similar to that of Ndt80-R177A (Figure 2-1A and C). In both of these strains, Cdc5 and Clb1 were not observed, suggesting an inability of the Ndt80-6D protein to mediate transcription of its middle gene targets, in a fashion similar to Ndt80-R177A.

The reduced level of Ndt80-6D protein is not due to protein instability

Our hypothesis is that the reduced levels of Ndt80-6D are due to the failure of the mutant protein to activate its own transcription and therefore only the *IME1*-dependent Ndt80-6D is observed. An alternative explanation is that the multiple aspartate residues destabilize the Ndt80-6D protein, resulting in its degradation. In this scenario, Ndt80-6D can transcribe *NDT80-6D* but the degradation of the destabilized protein results in lower than WT levels of protein. These two possibilities can be distinguished by expressing *NDT80-6D* in a manner that does not involve Ndt80 autoregulatory transcription. This goal can be achieved by ectopically expressing *NDT80-6D* under the control of a different promoter. In this situation, any changes in the quantity of Ndt80-6D would be a result of reduced protein stability and not due to changes in *NDT80-6D* expression.

Conditional *NDT80*-independent expression was achieved by placing the *NDT80* open reading frame (ORF) under the control of the *GAL1* promoter (P_{GAL1}) (Benjamin et al., 2003). The Gal4 transcriptional activator binds specifically to this promoter to activate transcription in the presence of galactose (Johnston, 1987). By fusing *GAL4* to a mammalian estrogen receptor (*GAL4-ER*), the addition of β-estradiol (ED) allows for expression of genes with the P_{GAL1} promoter (Benjamin et al., 2003). The ED-inducible allele of *NDT80* is referred to as *NDT80-IN* (Prugar et al., 2017). Using the New England Biolabs Gibson Assembly® method, the P_{GAL1} sequence was ligated upstream of the *NDT80* ORF and cloned into an integrative plasmid, pBG4. Plasmids containing P_{GAL1}*-NDT80,* P_{GAL1}*-ndt80-6A* or P_{GAL1}*-ndt80-6D*, (the latter two constructed by X. Chen) were transformed into two *ndt80*Δ *GAL4-ER* haploid strains of opposite mating type. The transformants were then mated to create a diploid strain reliant on ED for *NDT80-IN* expression and progression into the meiotic divisions.

Strains containing *NDT80-IN*, *ndt80-6A-IN*, or *ndt80-6D-IN* were transferred to Spo medium and incubated for 5 hours to allow cells to arrest in pachytene (Xu et al., 1995). After addition of ED, *NDT80-IN* and *ndt80-6A-IN* progressed through the meiotic divisions with similar kinetics, producing 87% and 81% asci, respectively (Figure 2-2A). The appearance of the Ndt80 and Ndt80-6A proteins at 6 hours correlated with the production of Cdc5 and Clb1 as well as entry into the meiotic divisions (Figure 2-2A and B). Both Ndt80 proteins were hyperphosphorylated, consistent with *IME2*-dependent phosphorylation that has been shown to promote Ndt80 activity (Sopko et al., 2002). Both proteins were almost completely degraded by 9 hours (Figure 2-2B and C).

In contrast to *ndt80-6D* transcribed using its own promoter, the Ndt80-6D protein was more abundant than Ndt80-6A at the 7 hour timepoint (Figure 2-2B and C). However, neither Cdc5 nor Clb1 were observed, in contrast to the WT and *ndt80-6A* strains (Figure 2-2B). Furthermore, Ndt80-6D protein was present at high levels for at least 10 hours, as expected given that the cells were arrested in meiotic prophase. Ndt80-6D accumulation was more pronounced through ectopic expression than it was through the endogenous *NDT80* promoter (Figure 3-2D). These results suggest that the aspartic acid mutations are not affecting Ndt80 function by destabilizing the protein, but instead are likely preventing Ndt80 from activating transcription of its targets, preventing the *NDT80* autoregulatory positive feedback loop.

Development of a live fluorescent imaging approach to monitor Ndt80 localization

Inactive Ndt80 has been reported to localize to the cytoplasm when the meiotic recombination checkpoint is active (Wang et al., 2011). If true, then cytoplasmic vs.

nuclear localization of Ndt80 should be controlled by Mek1 kinase activity. Testing this hypothesis requires being able to visualize Ndt80 in real time, which can be accomplished through live imaging analysis of a green fluorescent protein (GFP) tagged Ndt80. By expressing a *MEK1* allele (*mek1-as*) sensitive to inhibition by the purine analog 1-(1,1-dimethylethyl)-3-(1-napthalenyl)-1H-pyrazolo[3,4-d]pyrimidin-4-amine (1-NA-PP1), the checkpoint arrest in a *dmc1*Δ mutant can be alleviated to allow for meiotic progression (Wan et al., 2004). By inhibiting Mek1-as in *dmc1*Δ strains expressing fluorescently tagged Ndt80, changes in checkpoint-dependent Ndt80 localization could be monitored during a timecourse using fluorescence microscopy.

An initial attempt to fluorescently tag *NDT80* involved fusing three copies of GFP in frame to the 3' end of the ORF. This allele is referred to as *ndt80-3xGFP* (pBG3). The *ndt80-3xGFP* fusion was placed under the control of P_{GAL1}, resulting in *ndt80-3xGFP-IN* (pBG5), allowing ED-inducible production of Ndt80-3xGFP. The construct was introduced into two *dmc1*Δ *mek1-as* haploids of opposite mating type. One haploid expressed the *GAL4-ER* construct and the other expressed *HTB1-mORANGE*, which is histone 2B tagged with the fluorescent protein mOrange, to fluorescently mark the nucleus (the *HTB1-mORANGE* allele was provided by A. Neiman and cloned into the integrating plasmid used in this work by N. M. Hollingsworth). From these haploids, *dmc1*Δ *mek1-as HTB1-mORANGE* diploids were constructed that could also express either *NDT80-IN* or *ndt80-3xGFP-IN*.

The two diploids were transferred to Spo medium and incubated for five hours to synchronize them at the checkpoint arrest (Xu et al., 1995). After the addition of ED, 1-NA-PP1 was added to one half of the sporulating cultures, which were incubated to

allow for progression. The unrepaired DSBs in the *dmc1*Δ background trigger the meiotic recombination checkpoint arrest that is dependent upon Mek1 kinase activity (Xu et al., 1997) and little to no meiotic progression was observed in the *NDT80-IN* and *ndt80-3XGFP-IN* diploids after ED addition. In contrast, meiotic progression was observed when Mek1-as was inhibited, although the *ndt80-3XGFP-IN* diploid exhibited a significant delay compared to *NDT80-IN* (Figure 2-3A). After more than 24 hours in sporulation medium, cultures that were not exposed to 1-NA-PP1 did not sporulate (0%). While 26% of WT *NDT80-IN* cells sporulated after Mek1-as inhibition, the *ndt80-3xGFP-IN* culture with inhibitor did not sporulate, despite progressing through the meiotic divisions. Ndt80-3xGFP protein accumulation was greatly reduced compared to Ndt80 (Figure 2-3B). In addition, the *ndt80-3xGFP-IN* strain exhibited reduced levels of Cdc5 compared to the *NDT80-IN* strain. These results suggest that the C-terminal 3xGFP tagged Ndt80 protein is unstable, with a reduced ability to activate transcription of its target genes and thereby delaying meiotic progression.

An alternative approach to fluorescently tagging Ndt80 was employed that divides the GFP molecule into two components (Kamiyama et al., 2016) (Figure 2-4A). In this system, a GFP mutant missing the 11th, C-terminal, β-sheet (*GFP 1-10*) is constitutively expressed using the *TEF1* promoter (Partow et al., 2010). This protein does not fluoresce by itself, but it can if the eleventh β-sheet is supplied in *trans*. *NDT80-IN* containing five C-terminal copies of the 11th GFP β-sheet (*NDT80-5xβ11-IN*) was constructed using the Gibson Assembly® method. This plasmid was introduced into a diploid strain expressing *GFP1-10* and *HTB-mORANGE*.

To determine whether the two-component system worked to create fluorescent Ndt80 molecules, the diploids were grown to log phase in rich medium and expression of the *NDT80-IN* and *NDT80-5xβ11-IN* alleles were induced by ED. After incubating for three hours, the *NDT80-5xβ11-IN* strain had noticeable GFP fluorescence, which overlapped with the nuclear mOrange fluorescent signal (Figure 2-4B). This GFP fluorescence was not seen in cells expressing untagged Ndt80 or in *NDT80-5xβ11-IN* cells without the addition of ED. These results are consistent with the fact that *MEK1* is not expressed in vegetative cells and therefore, ectopically expressed Ndt80 would be predicted to localize to the nucleus (Rockmill and Roeder, 1991). Having shown that the two-component fluorescence system works to make fluorescent Ndt80, the next step will be to test this system in meiotic cells. These experiments were beyond the scope of this thesis.

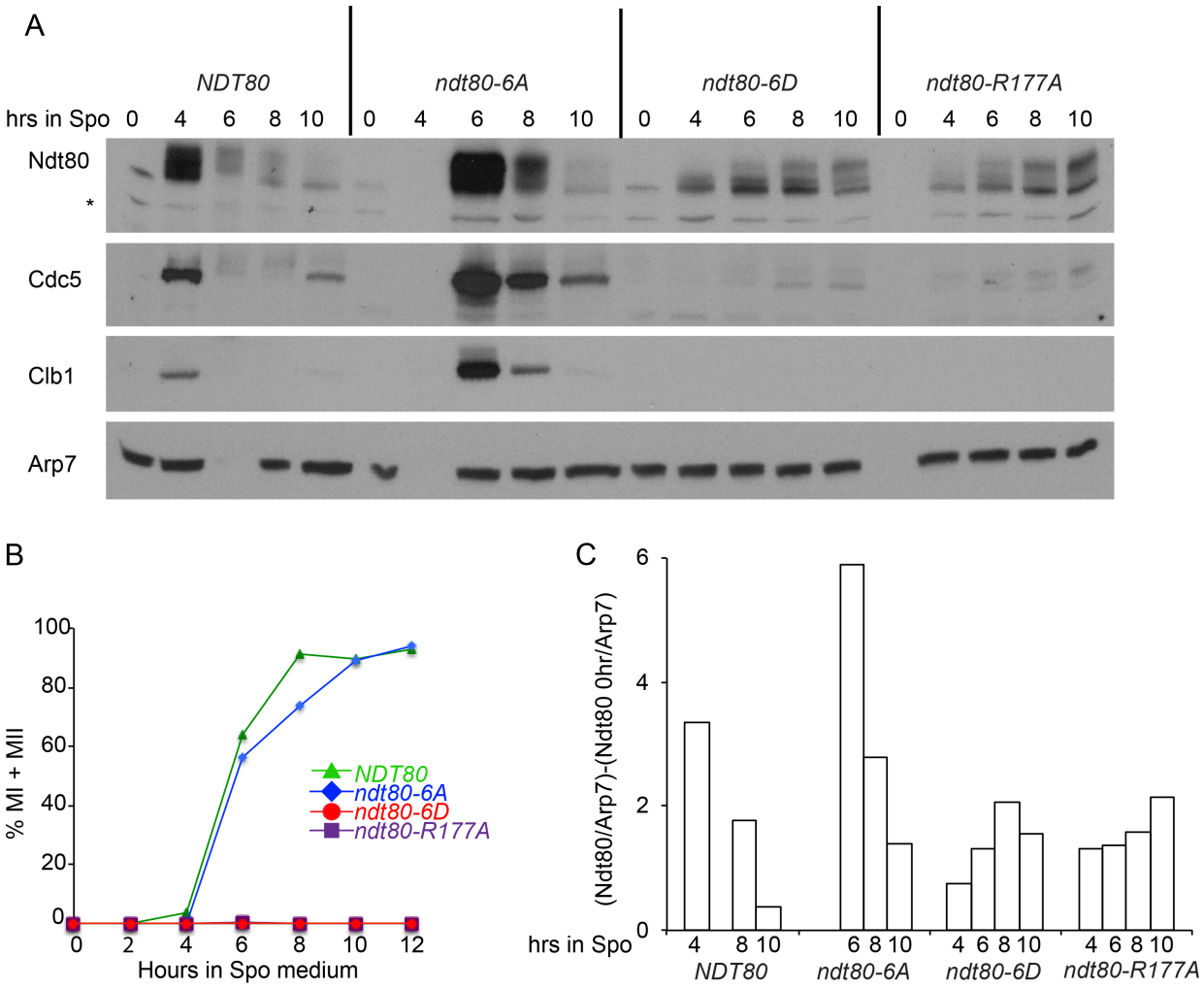

Figure 2-1. Negative charges on the DNA binding domain of Ndt80 prevent transcription of *NDT80*, *CDC5,* and *CLB1*. Strains expressing *NDT80* (NH2426::pEP105[2]::pHL8[2]), *ndt80-6A* (NH2426::pEP105[2]::pNH400[2]), *ndt80-6D* (NH2426::pEP105[2]::pNH401[2]), or *ndt80-R177A* (NH2426::pEP105[2]::pHL8-R177A[2]) were transferred to Spo medium to induce sporulation. (A) Immunoblot analysis of protein samples. The indicated proteins were detected using protein-specific antibodies. Arp7 was used as a loading control. Samples from the *NDT80* 6 hour, *ndt80-6A* 4 hour and *ndt80-R177A* 0 hour timepoints were lost during preparation of the extracts. The asterisk indicates a non-specific band. (B) Meiotic progression was determined by staining nuclei with DAPI and visualizing by fluorescence microscopy to monitor the completion of Meiosis I or Meiosis II (MI, MII, respectively). Samples were from the same timecourse as (A). Two hundred cells were counted per time point. (C) Quantification of Ndt80 immunoblots in (A). Ndt80 signals were normalized to their Arp7 signal and the normalized 0 hour signal was then subtracted from it.

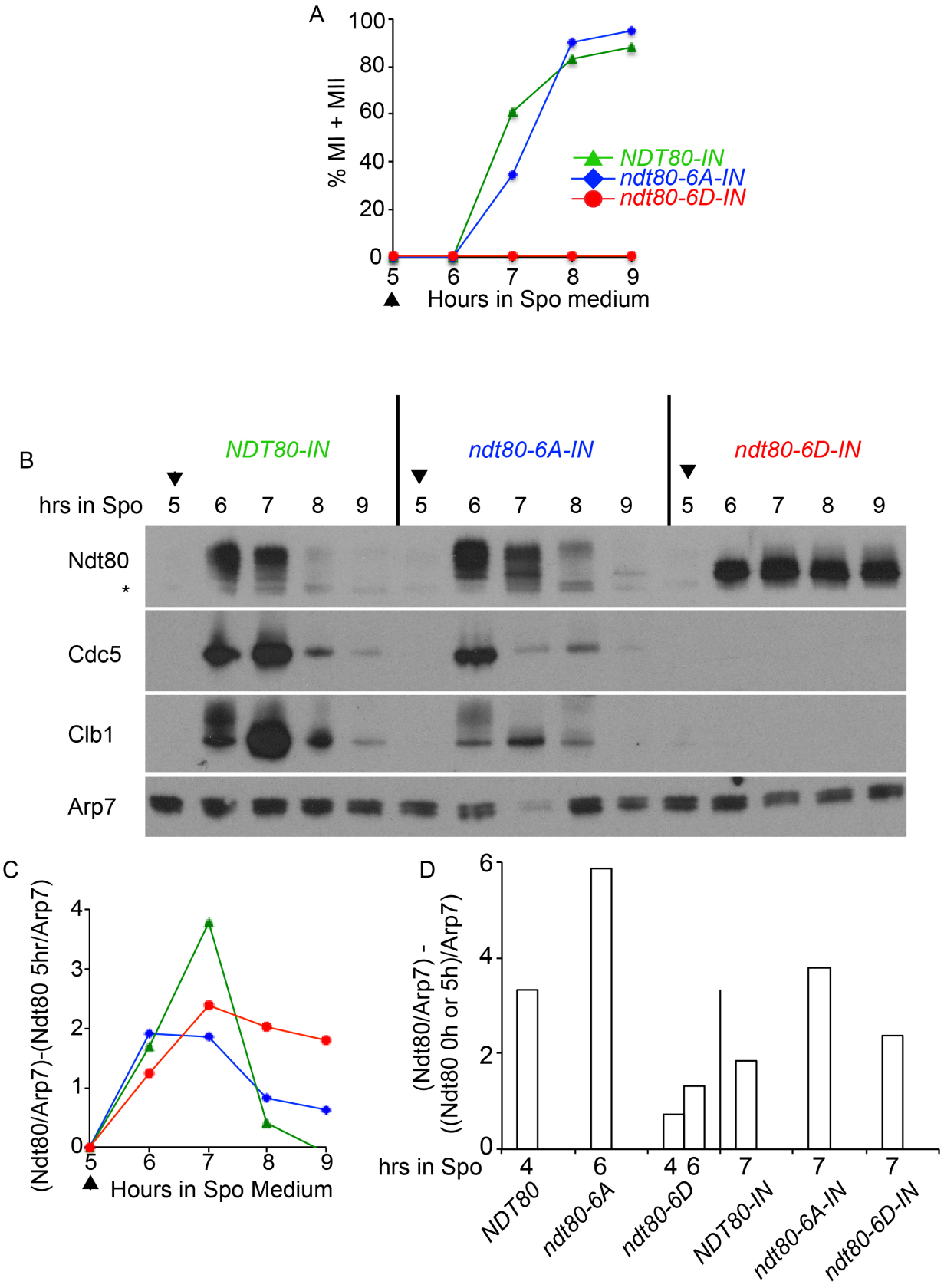
A
100
80
60
40
20
0
% MI + MII
NDT80-IN
ndt80-6A-IN
ndt80-6D-IN
5
6
7
8
9
Hours in Spo medium
B
NDT80-IN
ndt80-6A-IN
ndt80-6D-IN
hrs in Spo
5 6 7 8 9 5 6 7 8 9 5 6 7 8 9
Ndt80
*
Cdc5
Clb1
Arp7
C
(Ndt80/Arp7)-(Ndt80 5hr/Arp7)
4
3
2
1
0
5
6
7
8
9
Hours in Spo Medium
D
(Ndt80/Arp7) -
((Ndt80 0h or 5h)/Arp7)
6
4
2
0
hrs in Spo
4
6
4 6
7
7
7
NDT80
ndt80-6A
ndt80-6D
NDT80-IN
ndt80-6A-IN
ndt80-6D-IN

Figure 2-2. Negatively charged mutations in the Ndt80 DNA binding domain do not destabilize the protein. Strains expressing *NDT80-IN* (NH2426::pEP105^2::pBG4^2), *ndt80-6A-IN* (NH2426::pEP105^2::pXC11^2), or *ndt80-6D-IN* (NH2426::pEP105^2::pXC12^2) were transferred to Spo medium and incubated for five hours, at which time ED was added to a 1 micromolar (μM) final concentration to induce *NDT80* expression (arrowheads indicate time of ED addition). (A) Meiotic progression. Two hundred cells were counted per time point. (B) Immunoblot of protein samples taken from same timecourse as in (A). The indicated proteins were detected using protein-specific antibodies. Arp7 was used as a loading control. The asterisk indicates a non-specific band. (C) Quantification of Ndt80 immunoblots in (B). Ndt80 signals were normalized to their Arp7 signal and the normalized 5 hour signal was then subtracted from it. (D) Comparison of Ndt80 quantification from WT and P_{GAL1} promoters. Quantification of maximal timepoints of *NDT80, ndt80-6A,* and *ndt80-6D* strains from Figure 2-1C compared to those of *NDT80-IN, ndt80-6A-IN,* and *ndt80-6D-IN* strains from (C) in this figure. Normalizations are as shown in Figure 2-1C and Figure 2-2C, respectively.

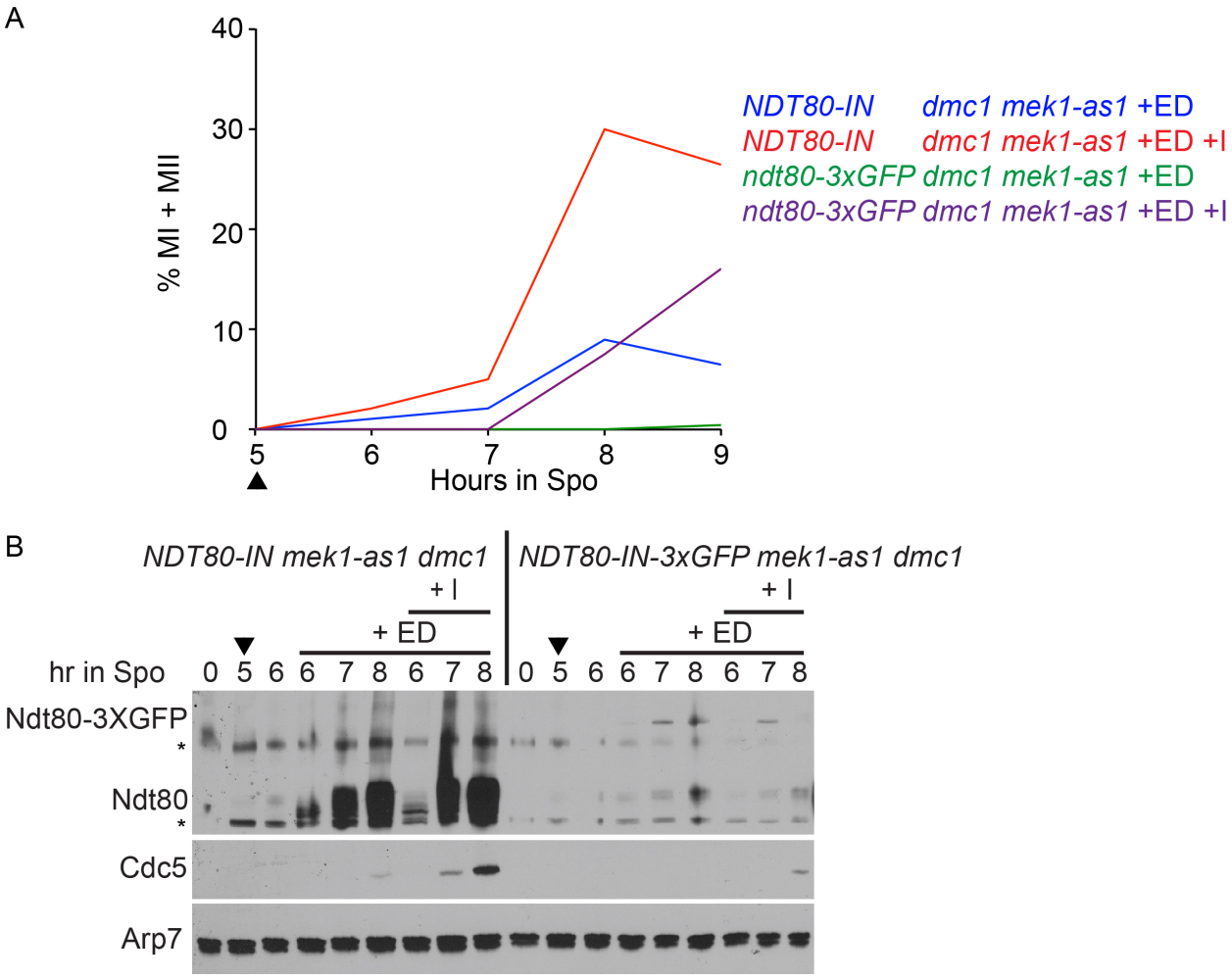

Figure 2-3. The Ndt80-3xGFP fusion protein is unstable. Diploids containing *dmc1*Δ *mek1-as* and either untagged or 3xGFP-tagged Ndt80 (NH2409::ENBG4[2] and NH2409::ENBG5[2]) were induced to sporulate in liquid Spo medium. Five hours after induction, 1 μM ED was added to the cultures to induce expression of *NDT80-IN* and *ndt80-3xGFP-IN*. Cultures were split between two flasks and 1 μM 1NA-PP1 (I) was added to one set of flasks to inhibit Mek1-as kinase activity (arrowheads indicate time of ED and 1-NA-PP1 addition). (A) Meiotic progression. Two hundred cells were counted per time point. (B) Protein samples were taken from same timecourse as (A) and immunoblotted with antibodies specific for Ndt80, Cdc5, and Arp7. Arp7 was used as a loading control. Asterisks correspond to non-specific bands.

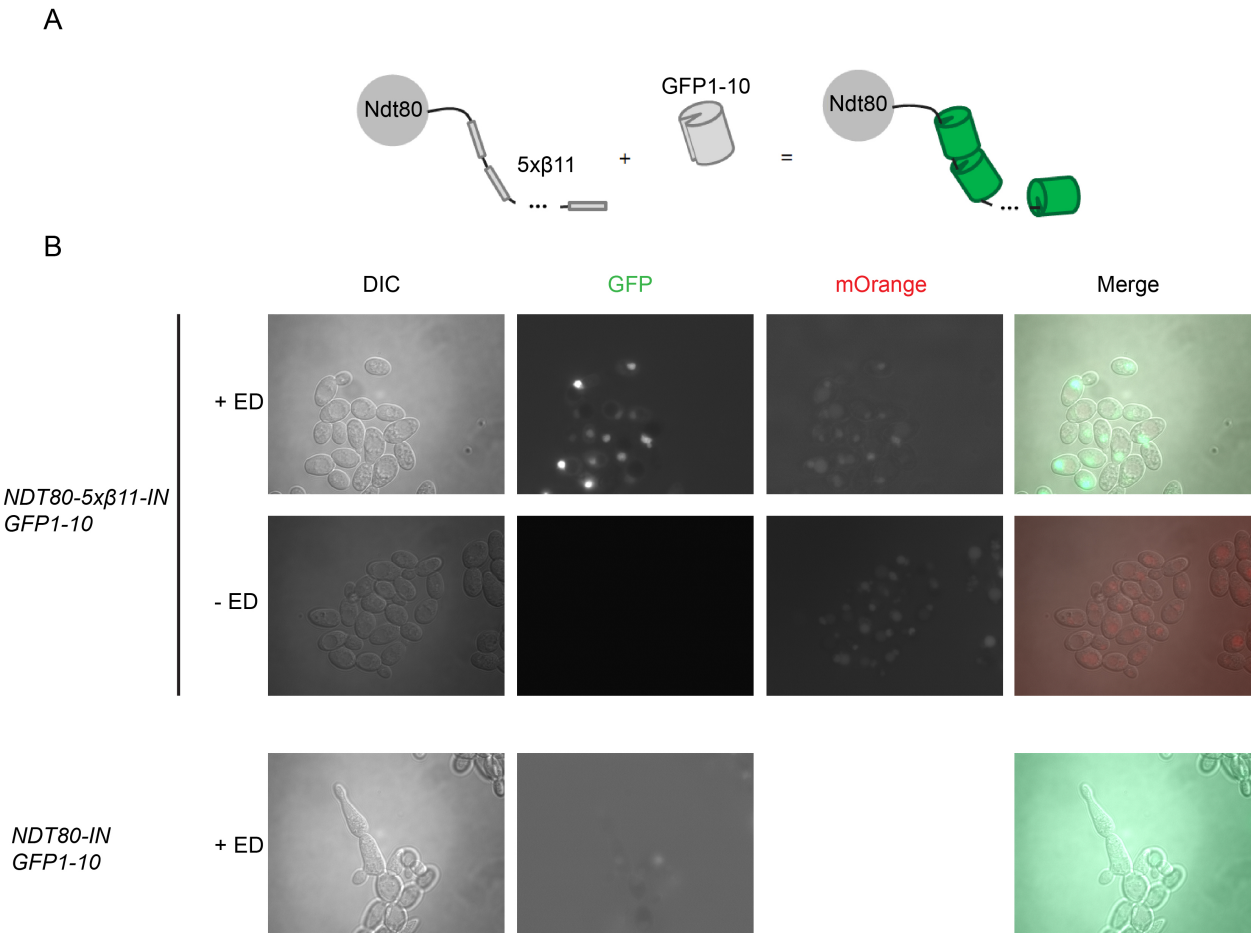

Figure 2-4. Simultaneous expression of *GFP1-10* and *NDT80-5xβ11-IN* allows for Ndt80-localized fluorescence in vegetative cells. (A) Diagram depicting the split GFP system (adapted from (Kamiyama et al., 2016)). The 5x β 11 tag was fused to the 3' end of the *NDT80* ORF. (B) Fluorescent imaging of live cell samples (NH2409::ENBG9^{2}BG10^2 and NH2409::ENBG9^{2}BG4^2). Cells were grown for 4.5 hours in rich medium and half of the cultures were exposed to 1 μM ED. Cells were grown for an additional 3 hours before viewing by fluorescence microscopy. DIC: differential interference contrast.

Discussion

Phosphorylation of Ndt80 DNA-binding domain prevents MSE association

Ndt80 is a meiosis-specific transcription factor involved in the expression of genes required for prophase exit and progression through the meiotic divisions (Chu and Herskowitz, 1998; Sourirajan and Lichten, 2008; Xu et al., 1995). To prevent Meiosis I divisions from occurring without proper homolog alignment, a recombination checkpoint prevents Ndt80 activity until Dmc1-mediated strand invasion allows for repair of DSBs using a homolog as the template (Dresser et al., 1997; Hepworth et al., 1998; Hong et al., 2001; Tung et al., 2000). The meiosis-specific checkpoint kinase Mek1 is activated by the formation of DSBs and acts through different substrates to promote interhomolog strand invasion and delay meiotic progression until all of the breaks have been repaired (Carballo et al., 2008; Lydall et al., 1996; Niu et al., 2007; Prugar et al., 2017; Rockmill and Roeder, 1991). Recent work from the Hollingsworth lab has indicated that Ndt80 is a direct substrate of Mek1.

Strains expressing the *ndt80-6A* DBD mutant progressed in a similar fashion as a WT strain, while the *ndt80-6D* strain showed no meiotic progression (Figure 2-1B). Protein extracts were probed for Ndt80 as well as Cdc5 and Clb1, the protein products of two of its downstream targets (Figure 2-1A). *ndt80-6A* strains appeared to accumulate more Ndt80 than WT (Figure 2-1C). Although direct comparison cannot be made between the two strains, this increased Ndt80 accumulation could be a result of the loss of a negative regulatory mechanism, allowing the Ime1-level Ndt80-6A to enhance *NDT80-6A* transcription immediately (Chu and Herskowitz, 1998). This would also lead to an enhanced expression of Ndt80-targeted genes, leading to a greater

accumulation of Cdc5 and Clb1 among other protein targets (Chu et al., 1998; Chu and Herskowitz, 1998), a phenotype that is apparent in this same immunoblot. The *ndt80-6D* strain had reduced levels of Ndt80-6D compared to both WT and *ndt80-6A* and no detectable accumulation of either downstream protein product (Figure 2-1A and C). This trend was similar to that seen from *ndt80-R177A* strains, which express a mutant unable to bind DNA (Montano et al., 2002). Ndt80-R177A protein cannot activate transcription of *NDT80*, so any accumulation is from Ime1-dependent transcripts. Therefore, the similarity in protein accumulation patterns between *ndt80-R177A* and *ndt80-6D* strains would suggest that the Ndt80-6D protein is similarly deficient in its ability to bind DNA, especially since the mutations are all in the DNA-binding domain.

However, the possibility could not be overlooked that the six aspartate mutations were destabilizing Ndt80-6D, leading to its degradation and reduced protein levels relative to WT or Ndt80-6A. By expressing *NDT80* mutants ectopically under the P_{GAL1} promoter, the autoregulatory *NDT80* expression loop was eliminated and *NDT80* expression could be normalized between strains (Benjamin et al., 2003). The considerable accumulation of Ndt80-6D compared to WT and the 6A mutant demonstrates that protein stability and degradation are not influencing protein production in any significant manner. Even with the Ndt80-6D accumulation provided by the ectopic expression system, the strain failed to accumulate detectable levels of either Cdc5 or Clb1 while WT and *ndt80-6A* strains readily accumulated both proteins (Figure 2-2B). This again suggests that the aspartate residues prevent the protein from activating transcription of its target genes.

Crystallographic analysis of the Ndt80 DBD has shown that at least four of the putative Mek1 substrates are located at the DNA-protein interface (Figure 1-1B) (Lamoureux et al., 2002). Positioning phosphate groups at these positions would likely repulse the negatively charged phosphate backbone of DNA, preventing Ndt80 from stably interacting with MSE sequences. Recent results by Trevor Leong have shown that mutating these DBD residues to neutrally charged but structurally similar asparagine residues does not affect sporulation (T. Leong, unpublished data), suggesting that negative charges at these positions are interfering with DNA binding. *In vitro* DNA-binding assays with recombinant Ndt80 WT and 5D DNA binding domains have confirmed this hypothesis (N. Hollingsworth, unpublished data).

The split GFP fluorescence system could be used to assay Ndt80 regulation and activity

Ndt80 protein is cytoplasmically localized as a result of checkpoint arrest (Wang et al., 2011). Visualization of Ndt80 localization in live sporulating cells would assist further study of this regulatory effect. This is most directly accomplished by fusing a fluorescent protein, such as GFP, to Ndt80. Changes in Ndt80 localization could then be monitored through the fluorescent signal of its tag. However, initial attempts at tagging the C-terminus of Ndt80 with three GFP molecules resulted in degradation of the fusion protein, perhaps due to the large size of the tag (Figure 2-3B). Some functional Ndt80-3xGFP protein was present in these strains that allowed for reduced Cdc5 accumulation and delayed meiotic progression. However, Ndt80 function was too compromised to be used for further studies.

Using the split GFP system adapted from (Kamiyama et al., 2016) allowed for Ndt80 localization to be monitored through its 5xβ11 tag. Unlike the Ndt80-3xGFP fusion, tagging Ndt80 with the smaller 5xβ11 sequence did not significantly affect protein stability. ED-induced *NDT80-5xβ11* expression produced enough protein for detectable nuclear fluorescence (Figure 2-4B). Since the induction occurred in vegetative cells, there was no Mek1 to affect Ndt80 localization, resulting in a "default" nuclear Ndt80 signal (Lydall et al., 1996; Rockmill and Roeder, 1991). Utilizing this system in sporulating *dmc1*Δ strains may allow for the visualization of the cytoplasmic localization described in (Wang et al., 2011) without requiring indirect immunofluorescence protocols (Bishop et al., 1992).

Active Mek1 kinase influences the ability of Ndt80 to function as a transcription factor (Tung et al., 2000; Wan et al., 2004). It is possible that Mek1 activity promotes the export of Ndt80 from the nucleus. If this hypothesis is correct, then inhibiting Mek1-as in *dmc1*Δ arrested cells expressing the fluorescence system should alter the localization pattern of Ndt80, resulting in primarily nuclear fluorescence corresponding to an alleviation of the arrest state and the start of meiotic progression (Xu et al., 1997). Recent studies, including results described above, also suggest that Mek1 phosphorylation of the Ndt80 DBD prevents stable binding to MSE sequences. It is possible that destabilizing the Ndt80-DNA interactions through DBD phosphorylation makes Ndt80 susceptible to a nuclear export mechanism, causing an increased cytoplasmic localization. The DNA binding ability mediated by the unphosphorylated DBD could allow Ndt80 to "anchor" itself to the MSEs, overcoming the nuclear export mechanism. This theory could be tested in part by using the fluorescent system to tag

Ndt80-R177A. If DNA-binding ability is sufficient to maintain nuclear localization, tagged Ndt80-R177A mutant should constitutively display a cytoplasmic fluorescent signal regardless of the state of the recombination checkpoint (Montano et al., 2002). If this proves to be the case, *ndt80-R177A* mutant strains could provide a useful control for future assays of Ndt80 activity. Additionally, other Ndt80 mutants, including the *ndt80-6A* and *-6D* alleles, could be fused to the 5xβ11 tag and their cellular localization could be analyzed in WT or *dmc1*Δ backgrounds. Monitoring Ndt80 cytoplasmic localization of these mutants could provide additional insight into Ndt80 regulation at the recombination checkpoint.

Methods

Media

The media used for this study contained the following ingredients:

LB + SOC liquid medium: lysogeny broth medium, super optimal broth with catabolite repression (0.4% glucose, 9.7 millimolar (mM) $MgSO_4$, 9.7mM $MgCl_2$)

LB + amp liquid medium: 1% tryptone, 0.5% yeast extract, 0.1% ampicillin

LB + amp solid medium: 2% agar, 1% tryptone, 1% NaCl, 0.5% yeast extract, 0.01% ampicillin

Synthetic defined (SD) solid medium: 2% agar, 0.7% yeast nitrogen base, 2% glucose, 0.2% dropout powder lacking various amino acids (contents of powder described in (Lo and Hollingsworth, 2011))

SD solid medium with 5-fluororotic acid (5-FOA): as above with: 0.2% complete powder (Lo and Hollingsworth, 2011) and 0.08% 5-FOA

Sporulation liquid medium (Spo): 2% potassium acetate

Sporulation solid medium: 1% potassium acetate, 0.1% yeast extract, 0.05% dextrose, 2% agar

YPA liquid medium: 2% peptone, 1% yeast extract, 2% potassium acetate

YPD liquid medium: 2% peptone, 1% yeast extract, 2% glucose

YPD com solid medium: 2% agar, 2% peptone, 1% yeast extract, 2% glucose, 0.2% complete powder

YPD com solid medium + G418: contains 0.02% Geneticin

YPD com solid medium + NAT: contains 0.02% Nourseothricin Sulfate

YPD com solid medium + HygB: contains 0.03% Hygromycin B

YP glycerol solid medium: 2% agar, 2% peptone, 1% yeast extract, 3% glycerol, 0.2% complete powder

Yeast strain construction

Strains used in this work are listed in Table 4-1.

All yeast strains were grown at 30 degrees Celsius (ºC). All strains used in this work were derived from the SK1 strain background, which sporulate rapidly and efficiently, making them useful for meiotic studies (Padmore et al., 1991). SK1 cells spontaneously accumulate mitochondrial mutations, leading to “petite” cells with a slow growth phenotype due to a loss of aerobic respiration processes, which also prevent them from sporulating (Ephrussi and Slonimski, 1955). Since petite cells cannot metabolize non-fermentable carbon sources, such as glycerol, all colonies were tested for growth on YP glycerol for 16 to 24 hours at 30°C. Colonies which grew using glycerol as the carbon source were “grande,” or non-petite, and used for experimentation.

To examine the phenotypes of various *NDT80* alleles in a *dmc1*Δ *mek1-as* background, it was first necessary to construct haploid strains containing *ndt80*Δ *mek1-as* and *dmc1*Δ. These strains also contained *trp1* and *ura3* as selectable markers for the integration of the *HTB1-mOrange* and *GAL4-ER* genes (both on *TRP1* plasmids), and various *NDT80* alleles carried on *URA3* plasmids (plasmids listed in Table 4-2). One haploid was derived from S2683 *ndt80 dmc1*Δ *mek1*Δ::pJR2 which contains a *URA3 mek1-as* plasmid integrated 700 basepairs (bp) downstream of the *mek1*Δ*::natMX4* locus. In this strain, the *MEK1* open reading frame (ORF) was deleted using the *natMX4*

gene, which confers resistance to NAT. Cells which lost the pJR2 plasmid by recombination were selected on plates containing 5-FOA, which is toxic to cells expressing the wild-type *URA3* gene (Boeke et al., 1987). Depending on where the crossover occurred, either the *mek1*Δ*::natMX4* or the *mek1-as* gene remained in the chromosome (Rothstein, 1991). S2683 *ndt80*Δ *mek1*Δ::pJR2 dmc1Δ cells were grown non-selectively overnight in YPD and then 10^{-2} and 10^{-3} dilutions were plated on SD + 5-FOA. Resistant colonies (5-Foa^{R}) were patched on YPDcom, grown overnight, and then replica plated to YPDcom + NAT plates to screen for NAT sensitive cells. These cells had lost the *mek1*Δ*::natMX4* sequence and therefore retained the *mek1-as* allele as a result of the pop-out. The resulting haploid was named S2683 *ndt80 mek1-as dmc1* Foa^{R} and frozen at -80ºC.

To allow for the integration of plasmids containing the *TRP1* gene as a selectable marker, the parental strain should lack of a functional *TRP1* gene, preventing them from growing on selectable plates lacking tryptophan. However, the strain should also have a sequence homologous to those at the ends of the linearized plasmid, to allow for an increased frequency of integration (Orr-Weaver et al., 1981). To accomplish this, the first 223 nucleotides of the *TRP1* gene in RKY1145 *mek1* were deleted (Chen et al., 2015). A 1.2 kilobase (kb) fragment was amplified from p4339 by polymerase chain reaction (PCR) using TRP1-5-nat-F1 and TRP1-5-nat-R1 as primers (Primer sequences are listed in Table 4-3). The resulting fragment contained *natMX4* flanked by 50 bp of homology to the *TRP1* locus. One end contained 50 bp immediately upstream of the *TRP1* ORF, while the other end was located from bp 224-274 within the *TRP1* ORF. The PCR fragment was precipitated with isopropanol, resuspended in 40 microliters

(μL) 1 X TE (0.1 Molar (M) Tris-HCl pH 7.4, 0.01M EDTA (ethylenediaminetetraacetic acid) pH 8) and 5 μL were transformed into RKY1145 *mek1*. Transformants were selected on YPDcom + NAT plates. Transformants were patched out onto YPDcom and, after overnight growth, transferred to SD-trp medium to confirm that the cells did not grow. The resulting haploid was named RKY1145 *mek1 trp1* and frozen at -80ºC.

S2683 *ndt80 mek1-as dmc1* Foa^R and RKY1145 *mek1 trp1* cells were mated on YPD overnight to make the diploid, NH2407, which was then replica plated to Spo plates and incubated for 24 hours. The resulting asci were dissected by Nancy Hollingsworth on YPDcom plates using a Zeiss tetrad dissecting microscope. The spore colonies were incubated at 30°C for 3 days. Due to independent assortment and recombination occurring during meiosis, the spore colonies were genotypically different from either parental strain. Cells containing the alleles indicated below were chosen by monitoring their growth after a 16 hour incubation at 30°C on various medium:

ndt80Δ::kanMX6 (G418 resistance)

mek1-as [leucine auxotrophy, screened against *mek1Δ::LEU2*]

trp1-5'Δ::natMX4 [tryptophan auxotrophy and NAT resistance]

dmc1-2EΔ::hphMX4 (*2EΔ*= second exon deletion) [Hygromycin B resistance]

ura3 [uracil auxotrophy].

Mating type tests were used to determine whether a haploid was *MAT***a** or *MAT*α. Spore colonies were replica plated to two YPD plates, onto which lawns of *MAT***a** *lys1* or *MATα lys1* cells were also replica plated. These tester strains are wild type for every gene except *LYS1*, making them auxotrophic for lysine. After allowing the cells to mate and grow overnight, they were replica plated to SD plates. Since the spore colonies

express *LYS1* but are auxotrophic for other metabolites, mating them to a *lys1* haploid strain of the opposite mating type results in diploid cells that can grow on the minimal SD medium. Growth on SD plates after mating to a tester of one mating type indicated that the spore colony was of the opposite mating type. By this method, genotypically correct haploids of both mating types were recovered, NH2407-35-3 and NH2407-58-3, and frozen at -80ºC.

Integrating plasmids were digested with a restriction enzyme to target recombination to a specific place in the yeast genome. The following plasmids were linearized for integration at the *URA3* locus using NsiI: pBG1, pBG3, pBG4, pBG5, pBG10, pHL8, pHL8-R177A, pNH400, pNH401, pXC11, pXC12, pRS306. For integration at the *TRP1* locus, pEP105 was linearized using NheI and pNH310 was linearized using BsgI. pBG9 was linearized with XcmI to target integration at the *LEU2* locus.

Correct plasmid integration was confirmed by colony PCR. Freshly grown yeast transformants were mixed in 30 µL 0.2% sodium dodecylsulfate (SDS) by vortexing for 15 seconds and then heated for 4 minutes on a 95°C heat block. The cells were pelleted by centrifugation and the supernatants were used for the PCR reactions. Each 50 µL reaction contained 3 µL of extracted DNA as well as 0.5 µL Choice-Taq™ DNA Polymerase (Denville Scientific), 5 µL 10x Taq buffer (Denville Scientific), 2 µL 25% Triton X-100, 2mM deoxynucleotide triphosphates (dNTPs), 29.5 µL deionized water (dH_2O), and 2.5 µL each of a set of primers. For plasmids containing *NDT80* under the control of its own promoter (pBG1, pBG3), TEST-NDT80 and NDT80-IN were used to generate a 600 bp product. Plasmids including the P_{GAL1}-*NDT80* gene (pBG4, pBG5,

pBG10) were amplified with GAL1-TEST and NDT80-IN to generate a 670 bp product. To confirm the presence of *GFP1-10* (pBG9), GFP1-10-IN and GFP1-10-OUT were used to generate an 890 bp product. *GAL4-ER* was amplified using ER-HBD-IN-REV and GAL4-SEQ7 as primers to generate a 693 bp product. Sequences of all oligonucleotides used are listed in Table 4-3. After an initial one minute denaturation at 95°C, the reactions underwent 35 cycles of denaturation, annealing, and elongation: 95°C for 30 seconds, 54°C for one minute, and 72°C for one minute. After a final 6-minute elongation, the sizes of the reaction products were confirmed by agarose gel electrophoresis. Integration of *HTB1-mOrange* was confirmed by monitoring red fluorescence at 40x magnification using an Axioskop 2 fluorescence microscope with a TEX-RED fluorescence filter.

To make *dmc1*Δ *mek1-as HTB1-mOrange GAL4-ER* diploids (NH2409::EN) with different *NDT80* alleles, NH2407-35-3::pNH310 and NH2407-58-3::pEP105 haploids expressing the same allele were mixed on YPDcom plates. To make *GAL4-ER* diploids (NH2426::pEP105[2]) with various *NDT80* alleles, SKY370 ndt80::pEP150 and SKY371 ndt80::pEP105 haploids were mixed on YPDcom plates. After an overnight 30°C incubation, the mixed cells were streaked onto a YPDcom plate and grown at 30°C for two days in order to grow single colonies. These cells were patched onto YPDcom and cross stamped with *MAT***a** *lys1* and *MATα lys1* mating tester strains and replica plated to SD. Non-mating diploids were screened due to their inability to mate and grow on SD medium.

Plasmids

Plasmids are listed in Table 4-2.

To make pBG1, containing the *NDT80* gene, a 4.4 kilobase (kb) fragment was amplified from the *URA3 NDT80* integrating plasmid, pHL8 (Lo et al., 2012), using NDT80-WT-EcoRI-F1 and NDT80-WT-ClaI-R1 as primers (Figure 4-1A). This fragment contains the *NDT80* gene with its promoter region and 3' untranslated region (UTR) flanked with 25 bp of homology immediately upstream of the EcoRI site of pRS306 and 25 bp of homology downstream of the Cla1 site of pRS306 (Sikorski and Hieter, 1989). This fragment was then combined with EcoRI/ClaI-digested pRS306 using the New England Biolabs Gibson Assembly® cloning kit and transformed into the *Escherichia coli* (*E. coli*) strain, DH5α. After isolating the plasmid using a Qiagen QIAprep® Spin Miniprep kit, the correct assembly of pBG1 was confirmed by digestion with XhoI, and the predicted 6.3 and 2.4 kb fragments were observed using a 0.8% 0.5 X Tris-Borate-EDTA (TBE) agarose gel. In addition, the plasmid was sent to the Stony Brook University DNA Sequencing Facility to confirm the correct sequence of the *NDT80* gene using the following primers: NDT80-SEQ1-F, NDT80-SEQ2-F, NDT80-SEQ3-F, NDT80-SEQ4-F, NDT80-SEQ5-R, and NDT80-SEQ6-F (Sequences listed in Table 4-3). In addition, the *NDT80* promoter region was sequenced using NDT80-SEQ7-R.

To make the *ndt80-3xGFP* construct (pBG3), the *NDT80* upstream region and open reading frame were amplified as a 4.0 kb fragment from pBG1 using NDT80-WT-EcoRI-F1 and NDT80-R1, with 5' homology to the final 25 bp of the pRS306 EcoRI digestion site (Figure 4-1B). The *3xGFP* gene was amplified as a 2.2 kb fragment from pFA6a-kanMX6-3xGFP (provided by Gang Zhao) using GFP-NDT80-F1 and 3xGFP-R1 with a 25 bp 5' homology to the 3' end of the *NDT80* ORF. The 3' UTR of *NDT80* was

amplified as a 395 bp fragment using NDT80-UTR-GFP-F1 and NDT80-WT-ClaI-R1. This fragment had 5' homology to the final 23 bp of *3xGFP* and 3' homology to the first 25 bp of the pRS305 ClaI digestion site. The fragments were ligated into EcoRI/ClaI-digested pRS306 using the Gibson Assembly® kit and transformed into *E. coli*. Proper construction of the plasmid was confirmed by digesting with NotI and SalI, and observing the predicted 6.6 and 4.3 kb bands. The *NDT80-3xGFP* gene was sequenced and confirmed to be correct. In addition to primers for the *NDT80* ORF and the *NDT80* promoter region, the *3xGFP* gene was sequenced with 3xGFP-SEQ1-F, 3xGFP-SEQ2-F, 3xGFP-SEQ3-F, and 3xGFP-SEQ4-R.

To make the P_{GAL1}-*NDT80* construct (pBG4), the *GAL1* promoter (P_{GAL1}) sequence was amplified from pFA6a-HisMX6-PGAL1-GFP (Longtine et al., 1998) using pGAL1-EcoRI-F1 and pGAL1-R1 to produce a 441 bp fragment with 5' homology to the last 25 bp of the pRS306 EcoRI cut site (Figure 4-1C). The *NDT80* ORF and 3' UTR were amplified from pBG1 using NDT80-ORF-GAL1-F1 and NDT80-WT-ClaI-R1 to produce a 2234 bp fragment with a 31 bp 5' homology to the 3' end of the P_{GAL1} fragment and a 25 bp 3' homology to the pRS306 ClaI cut site. The two fragments were ligated into EcoRI/ClaI digested pRS306 using the Gibson Assembly® kit and transformed into *E. coli*. The correct assembly of pBG4 was confirmed by digesting miniprep plasmid DNA with NotI and EcoRI, and observing the expected 4.6, 1.4, and 1.0 kb products. The P_{GAL1}-*NDT80* gene in pBG4 was sequenced and confirmed to be correct using primers for sequencing the *NDT80 ORF*.

To make pBG5 (P_{GAL1}-*ndt80-3xGFP*), a 4.4 kb fragment containing *ndt80-3xGFP* was amplified from pBG3 using NDT80-ORF-GAL1-F1 and NDT80-WT-ClaI-R1 (Figure

4-1D). This fragment had 25 bp of 5' homology to the 3' end of the P_{GAL1} sequence and 25 bp of 3' homology to the pRS306 ClaI cut site. This fragment and the 441 bp P_{GAL1} fragment (described above) were ligated into EcoRI/ClaI-digested pRS306 using the Gibson Assembly® kit and transformed into *E. coli.* The isolated plasmid was digested with NotI and EcoRI, and the expected 4.6, 3.3, and 1.4 kb fragments were observed. The P_{GAL1}-*ndt80-3xGFP* gene in pBG5 was sequenced and confirmed to be correct using primers for sequencing the *NDT80 ORF* and *3xGFP*.

The pRS425-TEF1-GFP1-10-IDT plasmid, provided by Yuping Chen, contains the *GFP1-10* gene under the control of the constitutive *TEF1* promoter and the *CYC1* terminator (P_{TEF1}-*GFP1-10*-T_{CYC1}) (Curran et al., 2013; Partow et al., 2010). It also contains the 2μ plasmid origin of replication so that is can replicate autonomously. Since the sporulation induction process involves growth in non-selective medium, the plasmid can be lost. By cloning the P_{TEF1}-*GFP1-10*-T_{CYC1} gene into the *LEU2* integrating vector, pRS305, to make pBG9, the chance for the spontaneous loss of the plasmid was reduced (Figure 4-1E). The P_{TEF1}-*GFP1-10*-T_{CYC1} gene contained within a 1.7 kb SacI/NgoMIV fragment from pRS425-TEF1-GFP1-10-IDT was subcloned into SacI/NgoMIV digested pRS305 (Sikorski and Hieter, 1989). The fragment and vector backbone were purified from a 0.8% 0.5X Tris-acetic acid-EDTA (TAE) agarose gel using the Qiagen QIAquick® Gel Extraction Kit. The fragments were ligated together using T4 DNA ligase and transformed into *E. coli*. The presence of the insert was confirmed by digesting transformant plasmid DNA with SacI and NgoMIV, and observing the predicted 5.2 and 1.2 kb products.

To make P_{GAL1}-*ndt80-5xβ11* (pBG10), the P_{GAL1}-*NDT80* ORF sequence from pBG4 was amplified using pGAL1-EcoRI-F1 and NDT80-R1 to produce a 2.3 kb fragment with 25 bp of 5' homology to the pRS306 EcoRI cut site (Figure 4-1F). The *5xβ11* tag was amplified from pRS425-GAL1-sc5xGFP11 (provided by Yuping Chen) using NDT80-5xGFP11-F1 and 5xGFP11-R1 to produce a 445 bp fragment with 25 bp of 5' homology to the 3' end of the *NDT80* ORF. The *NDT80* 3' UTR was amplified from pBG4 using 5xGFP11-NDT80-UTR-F1 and NDT80-WT-ClaI-R1, generating a 399 bp fragment with 25 bp of 5' homology to the 3' end of the *5xβ11* tag and 25 bp of 3' homology to the pRS306 ClaI digestion site. The fragments were combined into EcoRI/ClaI digested pRS306 using the Gibson Assembly® kit and transformed into *E. coli*. The plasmid was isolated and digested with NotI and SalI, which produced the expected 4.3 and 3.1 kb products. The P_{GAL1}-*ndt80-5xβ11* gene in pBG10 was sequenced and confirmed to be correct using primers for the *NDT80 ORF*.

Timecourses

Yeast diploid strains were induced to sporulate as described in (Lo and Hollingsworth, 2011). For NH2426-derived strains, 0.3 milliliters (mL) of overnight culture was diluted into 250 mL YPA in a 1 liter (L) flask or 0.4 mL culture was diluted into 500 mL of YPA in a 2 L flask. For NH2409-derived strains, 0.6 mL of overnight culture was diluted into 200 mL of YPA in a 2 L flask. Samples were taken at various timepoints to analyze proteins as well as meiotic progression. For protein analysis, five mL of culture were placed in 15 mL conical tubes, the cells pelleted for 5 minutes in an IEC Clinical Centrifuge at 1040 x g and frozen at -80°C. To monitor meiotic

progression, 0.5 mL of culture were fixed with 3.7% formaldehyde and stored at 4°C. Cultures were sporulated at 30°C in a 250 revolutions per minute (RPM) shaker in Spo using ≥ 1:5 culture : flask volume ratio. For sporulating cultures with P_{GAL1}-*NDT80* constructs, β-estradiol was added from a 5 mM stock (in ethanol) for a 1 μM final concentration to induce transcription of *NDT80* alleles from the P_{GAL1} promoter. To inhibit Mek1-as kinase activity, the purine analog, 1-(1,1-dimethylethyl)-3-(1-napthalenyl)-1H-pyrazolo[3,4-d]pyrimidin-4-amine (1-NA-PP1) was added from a 10 mM stock (in dimethylsulfoxide) for a 1 μM final concentration to one half of the sporulation culture. After at least 24 hours, 200 cells were counted from each culture to determine the percent sporulation. Mature asci were considered as sporulated cells.

Meiotic Progression

Cells fixed in formaldehyde solution were spotted on microscope slides, washed three times with dH_2O and exposed to VECTASHIELD® mounting medium with 4',6-diamidino-2-phenylindole (DAPI). Cell nuclei were viewed at 40x magnification using an Axioskop 2 fluorescent microscope and a DAPI fluorescence filter. 200 cell nuclei were counted per sample. Cells with two nuclei (binucleate) have completed Meiosis I (MI), while cells with four nuclei (tetranucleates) have completed Meiosis II (MII).

Vegetative induction of P_{GAL}-*NDT80-5xβ11* and cytological analysis using fluorescence microscopy

Strains were inoculated in 4 mL YPD and incubated at 30°C for 19 hours. The cultures were diluted into 100 mL YPD and incubated on a shaker at 30°C at 250 RPM

for 4.5 hours. The optical density at 660 nanometers (nm) (OD_{660}) was taken and the cultures were harvested as described in (Lo and Hollingsworth, 2011). The cells were resuspended in YPD for a cell density of $3x10^7$ cells/mL and the volumes between cultures were made equal. The cultures were split between two flasks and β-estradiol (ED) was added to one half of the cultures, which were then grown for three additional hours on a shaker at 30°C and 250 RPM.

Live cell samples were taken from liquid cell cultures and kept on ice or at 4°C. Samples were spotted on microscope slides and visualized at 100 x magnification using an AXIO Observer.Z1 fluorescence microscope. A HAL 100 halogen lamp was used to visualize cells using differential interference contrast (DIC). GFP fluorescence was monitored using a Colibri.2 LED light source and a fluorescein isothiocyanate (FITC) filter (480 nm excitation filter, 535 nm emission filter). mOrange fluorescence was monitored using an external HXP 120 volt light source set for a 555 nm emission wavelength and a rhodamine filter (540 nm excitation filter, 605nm emission filter).

Protein extraction and immunoblot

Pellets of timecourse cell samples were resuspended in 5 mL of trichloroacetic acid (TCA). Protein samples were extracted as described in (Falk et al., 2010). Samples were fractionated and transferred to polyvinylidine difluoride (PVDF) membranes as described in (Prugar et al., 2017). Primary and secondary antibodies used in this work are listed in Table 4-4.

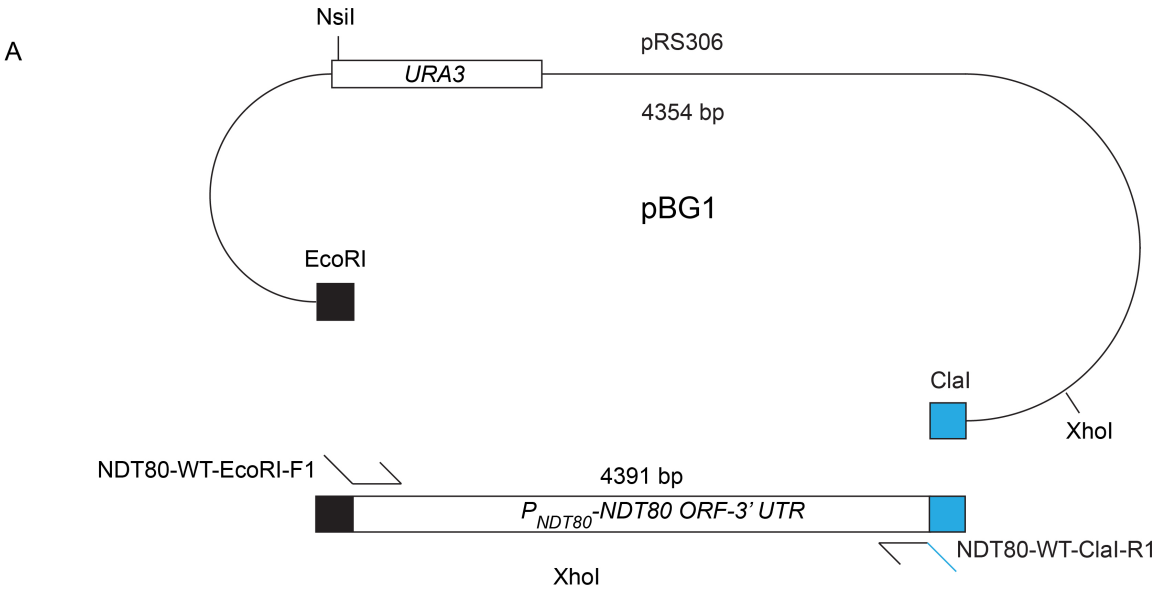
A
NsiI
URA3
pRS306
4354 bp
pBG1
EcoRI
ClaI
XhoI
NDT80-WT-EcoRI-F1
4391 bp
P NDT80-NDT80 ORF-3' UTR
NDT80-WT-ClaI-R1
XhoI

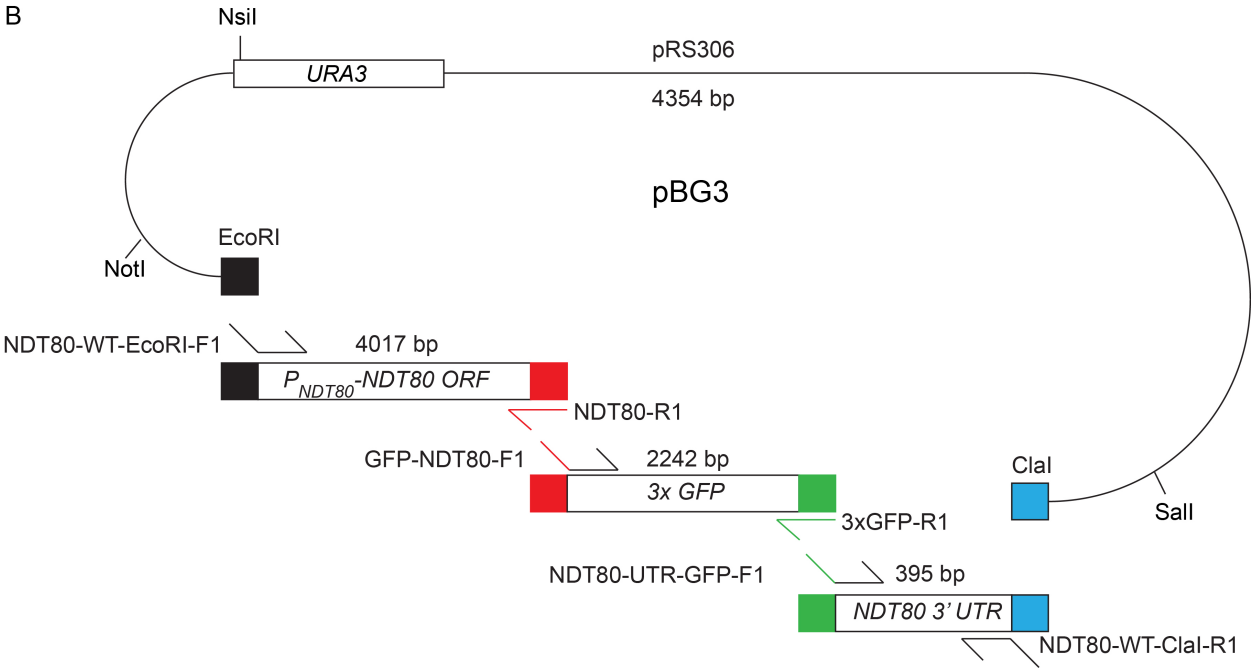
B
NsiI
URA3
pRS306
4354 bp
pBG3
EcoRI
NotI
NDT80-WT-EcoRI-F1
4017 bp
P NDT80-NDT80 ORF
NDT80-R1
GFP-NDT80-F1
2242 bp
3x GFP
ClaI
SalI
3xGFP-R1
NDT80-UTR-GFP-F1
395 bp
NDT80 3' UTR
NDT80-WT-ClaI-R1

C

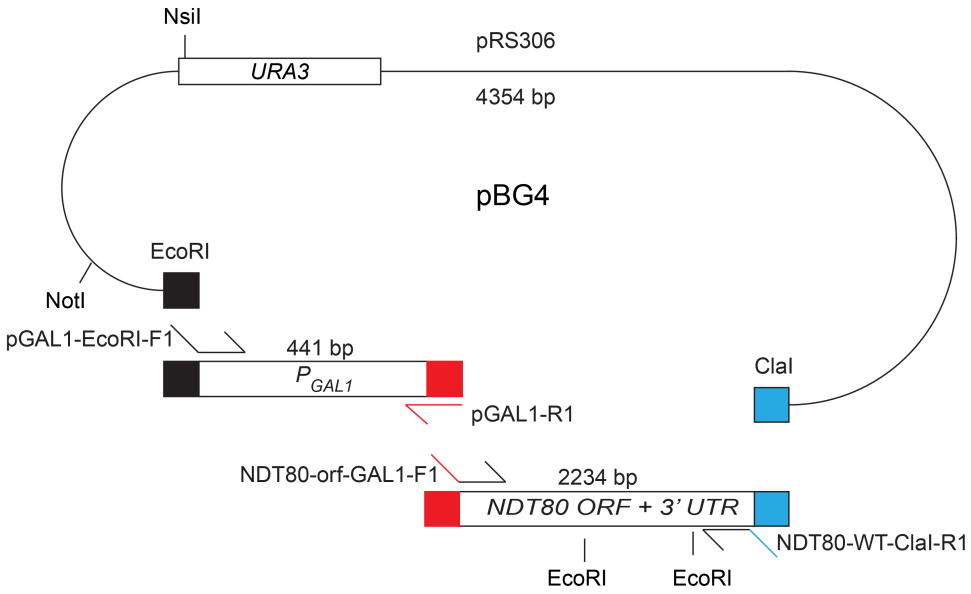
NsiI
URA3
pRS306
4354 bp
pBG4
EcoRI
NotI
pGAL1-EcoRI-F1
441 bp
P_{GAL1}
pGAL1-R1
ClaI
NDT80-orf-GAL1-F1
2234 bp
NDT80 ORF + 3' UTR
NDT80-WT-ClaI-R1
EcoRI
EcoRI

D

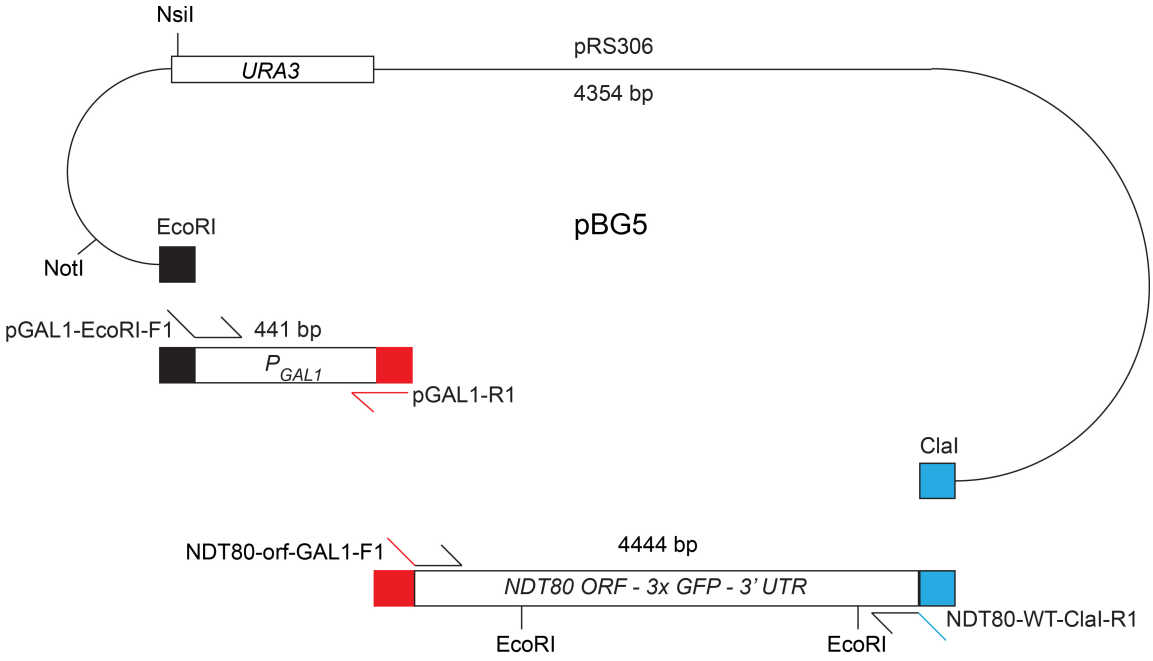
NsiI
URA3
pRS306
4354 bp
pBG5
EcoRI
NotI
pGAL1-EcoRI-F1
441 bp
P_{GAL1}
pGAL1-R1
ClaI
NDT80-orf-GAL1-F1
4444 bp
NDT80 ORF - 3x GFP - 3' UTR
NDT80-WT-ClaI-R1
EcoRI
EcoRI

E

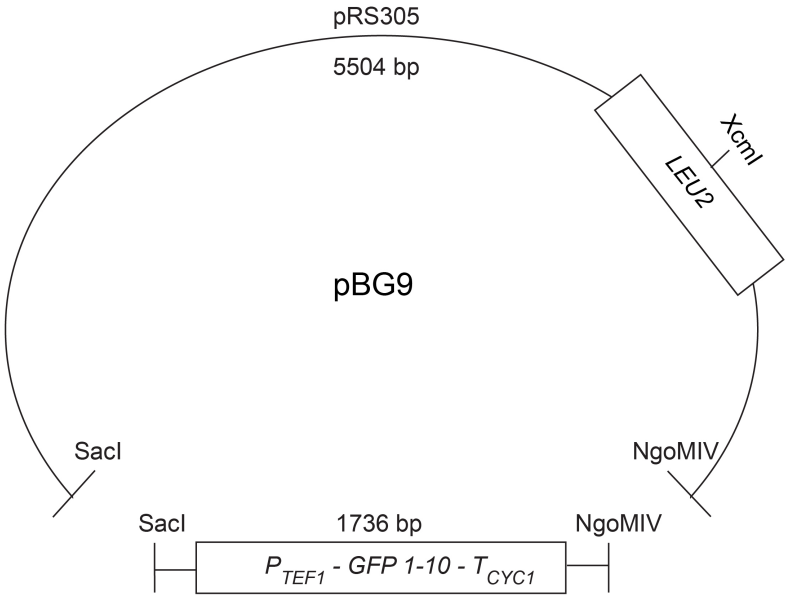
pRS305
5504 bp
XcmI
LEU2
pBG9
SacI
NgoMIV
SacI
1736 bp
NgoMIV
P_{TEF1} - GFP 1-10 - T_{CYC1}

F

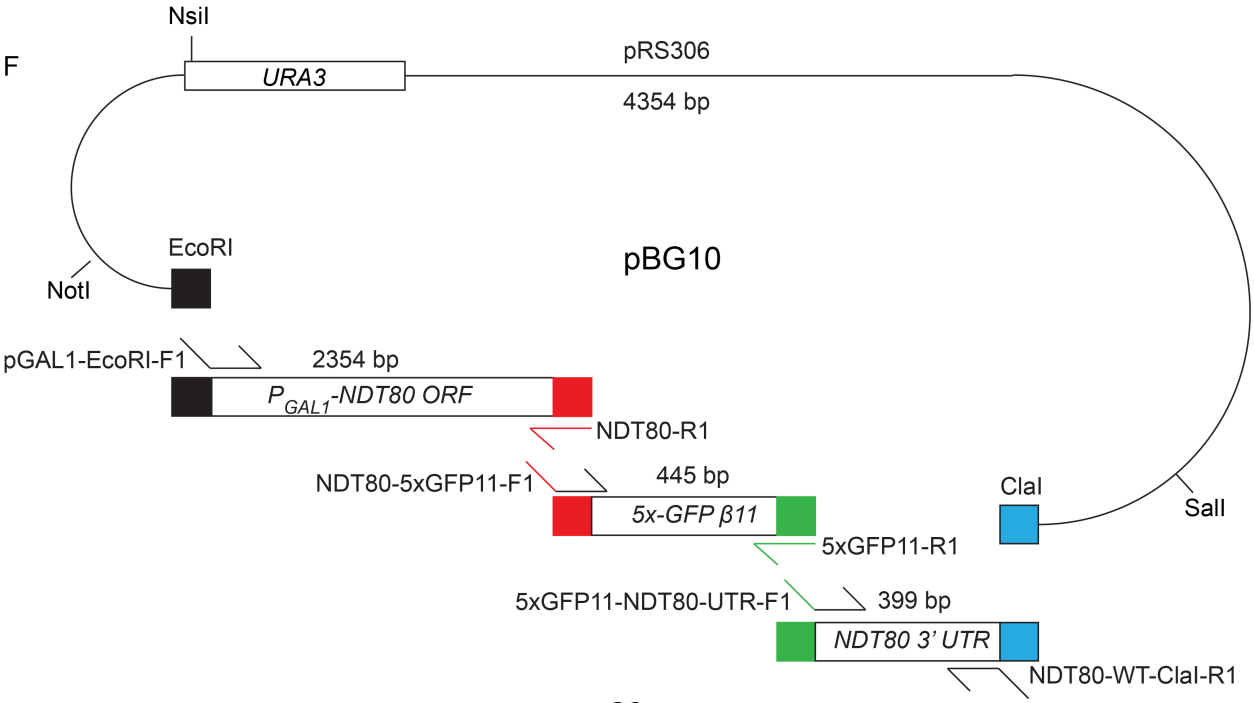
NsiI
URA3
pRS306
4354 bp
EcoRI
NotI
pBG10
pGAL1-EcoRI-F1
2354 bp
P_{GAL1}-NDT80 ORF
NDT80-R1
NDT80-5xGFP11-F1
445 bp
5x-GFP β11
ClaI
SalI
5xGFP11-R1
5xGFP11-NDT80-UTR-F1
399 bp
NDT80 3' UTR
NDT80-WT-ClaI-R1

Figure 4-1. Gibson Assembly plasmid construction strategies. Colored sequences represent homologous sequences between two fragments. Colored flaps of primers represent sequences that are not homologous to the template sequence but resulted in homology for the fragment. Fragment amplification and templates are described in Materials and Methods. Sequences of the oligonucleotides are listed in Table 4-3. (A) pBG1. (B) pBG3. (C) pBG4. (D) pBG5. (E) pBG9. (F) pBG10. Flat ends in (E) represent restriction enzyme cut sites.

Table 4-1. Yeast strains

Name	Genotype	Source
RKY1145 mek1	*MAT***a** *leu2ΔhisG his4-x ura3 lys2 mek1Δ::LEU2*	(de los Santos et al., 2001)
RKY1145 mek1 trp1	*MAT***a** *leu2ΔhisG his4-x ura3 lys2 mek1Δ::LEU2 hoΔLYS2 trp1-5'Δ::natMX4*	This work
S2683 ndt80 mek1∆::pJR2 dmc1	*MATα leu2-k arg4-Nsp ura3 lys2 ho::LYS2 ndt80Δ::kanMX6 mek1Δ::natMX4::URA3::mek1-as1 dmc1-2EΔ::hphMX4*	David Chen
S2683 ndt80 mek1-as dmc1 Foa^R	*MATα leu2-k arg4-Nsp ura3 lys2 ho::LYS2 ndt80Δ::kanMX6 mek1-as dmc1-2EΔ::hphMX4*	This work
NH2407	*MATα leu2-k HIS4 arg4-Nsp ura3 lys2 hoΔ::LYS2* *MAT***a** *leu2ΔhisG his4-x ARG4 ura3 lys2 hoΔ::LYS2* *ndt80Δ::kanMX6 mek1Δ::LEU2* *NDT80 mek1-as* *DMC1 trp1-5'Δ::natMX4* *dmc1-2EΔ::hphMX4 TRP1*	This work
NH2407-35-3	*MATα leu2 arg4-Nsp ura3 lys2 hoΔ::LYS2 ndt80Δ::kanMX6 mek1-as* *dmc1-2EΔ::hphMX4 trp1-5'Δ::natMX4*	This work
NH2407-35-3::pNH310	Same as NH2407-35-3 except *trp1-5'Δ::natMX4::HTB1-MORANGE::TRP1*	This work

NH2407-35-3::pNH310::pBG4	Same as NH2407-35-3 except *trp1-5'Δ::natMX4::HTB1-MORANGE::TRP1 ura3::P_{GAL1}-NDT80::URA3*	This work
NH2407-35-3::pNH310::pBG5	Same as NH2407-35-3 except *trp1-5'Δ::natMX4::HTB1-MORANGE::TRP1 ura3::P_{GAL1}-ndt80-3xGFP::URA3*	This work
NH2407-35-3::pNH310::pBG9	Same as NH2407-35-3 except *trp1-5'Δ::natMX4::HTB1-MORANGE::TRP1 leu2::GFP1-10::LEU2*	This work
NH2407-35-3::pNH310::pBG9::pBG10	Same as NH2407-35-3 except *trp1-5'Δ::natMX4::HTB1-MORANGE::TRP1 leu2::GFP1-10::LEU2* *ura3::P_{GAL1}-NDT80-5xβ11::URA3*	This work
NH2407-35-3::pNH310::pBG9::pBG4	Same as NH2407-35-3 except *trp1-5'Δ::natMX4::HTB1-MORANGE::TRP1 leu2::GFP1-10::LEU2* *ura3::P_{GAL1}-NDT80::URA3*	This work
NH2407-58-3	*MAT**a** leu2 his4-x arg4-Nsp ura3 lys2 hoΔ::LYS2 ndt80Δ::kanMX6 mek1-as dmc1-2EΔ::hphMX4 trp1-5'Δ::natMX4*	This work
NH2407-58-3::pEP105	Same as NH2407-58-3 except *trp1-5'Δ::natMX4::GAL4-ER::TRP1*	This work

NH2407-58-3::pEP105::pBG4	Same as NH2407-58-3 except *trp1-5'Δ::natMX4::GAL4-ER::TRP1 ura3::P_{GAL1}-NDT80::URA3*	This work
NH2407-58-3::pEP105::pBG5	Same as NH2407-58-3 except *trp1-5'Δ::natMX4::GAL4-ER::TRP1 ura3::P_{GAL1}-ndt80-3xGFP::URA3*	This work
NH2407-58-3::pEP105::pBG9	Same as NH2407-58-3 except *trp1-5'Δ::natMX4::GAL4-ER::TRP1 leu2::GFP1-10::LEU2*	This work
NH2407-58-3::pEP105::pBG9::pBG10	Same as NH2407-58-3 except *trp1-5'Δ::natMX4::GAL4-ER::TRP1 leu2::GFP1-10::LEU2* *ura3::P_{GAL1}-NDT80-5xβ11::URA3*	This work
NH2407-58-3::pEP105::pBG9::pBG4	Same as NH2407-58-3 except *trp1-5'Δ::natMX4::GAL4-ER::TRP1 leu2::GFP1-10::LEU2* *ura3::P_{GAL1}-NDT80::URA3*	This work

NH2409	*MATα leu2 HIS4 arg4-Nsp ndt80Δ::kanMX6* *MAT**a** leu2 his4-x arg4-Nsp ndt80Δ::kanMX6* *ura3 dmc1-2EΔ::hphMX4 lys2 hoΔ::LYS2* *ura3 dmc1-2EΔ::hphMX4 lys2 hoΔ::LYS2* *mek1-as trp1-5'Δ::natMX4* *mek1-as trp1-5'Δ::natMX4*	This work
NH2409::EN = NH2409::pEP105::pNH310	Same as NH2409 except *trp1-5'Δ::natMX4::htb1-mOrange::TRP1* *trp1-5'Δ::natMX4::GAL4-ER::TRP1*	This work

NH2409::EN BG4[2]	Same as NH2409 except *trp1-5'Δ::natMX4:: HTB1-MORANGE::TRP1* *trp1-5'Δ::natMX4::GAL4-ER::TRP1* *ura::P_{GAL1}-NDT80::URA3* *ura::P_{GAL1}-NDT80::URA3*	This work
NH2409::EN BG5[2]	Same as NH2409 except *trp1-5'Δ::natMX4:: HTB1-MORANGE::TRP1* *trp1-5'Δ::natMX4::GAL4-ER::TRP1* *ura::P_{GAL1}-ndt80-3xGFP::URA3* *ura::P_{GAL1}-ndt80-3xGFP::URA3*	This work
NH2409::EN BG9[2]BG10[2]	Same as NH2409 except *leu2::GFP1-10::LEU2 ura3:: P_{GAL1}-NDT80-5xβ11::URA3* *leu2::GFP1-10::LEU2 ura3:: P_{GAL1}-NDT80-5xβ11::URA3* *trp1-5'Δ::natMX4:: HTB1-MORANGE::TRP1* *trp1-5'Δ::natMX4::GAL4-ER::TRP1*	This work
NH2409::EN BG9[2]BG4[2]	Same as NH2409 except *leu2::GFP1-10::LEU2 ura3:: P_{GAL1}-NDT80::URA3* *leu2::GFP1-10::LEU2 ura3:: P_{GAL1}-NDT80::URA3* *trp1-5'Δ::natMX4::HTB1-MORANGE::TRP1* *trp1-5'Δ::natMX4::GAL4-ER::TRP1*	This work

NH2426	*MAT**a** leu2::hisG his4B::LEU2 trp1::hisG* *MATα leu2::hisG his4X::LEU2 trp1::hisG* *arg4-Bgl ndt80::hphMX4 ho::LYS2 lys2 ura3* *arg4-nsp ndt80::hphMX4 ho::LYS2 lys2 ura3*	This work
NH2426::pEP105[2]	Same as NH2426 except *trp1::hisG::GAL4-ER::TRP1* *trp1::hisG::GAL4-ER::TRP1*	This work
NH2426::pEP105[2]::pBG4[2]	Same as NH2426 except *trp1::hisG::GAL4-ER::TRP1 ura3::P_{GAL1}-NDT80::URA3* *trp1::hisG::GAL4-ER::TRP1 ura3::P_{GAL1}-NDT80::URA3*	This work
NH2426::pEP105[2]::pHL8[2]	Same as NH2426 except *trp1::hisG::GAL4-ER::TRP1 ura3::NDT80::URA3* *trp1::hisG::GAL4-ER::TRP1 ura3::NDT80::URA3*	This work
NH2426::pEP105[2]::pHL8-R177A[2]	Same as NH2426 except *trp1::hisG::GAL4-ER::TRP1 ura3::ndt80-R177A::URA3* *trp1::hisG::GAL4-ER::TRP1 ura3::ndt80-R177A::URA3*	This work
NH2426::pEP105[2]::pNH400[2]	Same as NH2426 except *trp1::hisG::GAL4-ER::TRP1 ura3::ndt80-6A::URA3* *trp1::hisG::GAL4-ER::TRP1 ura3::ndt80-6A::URA3*	This work
NH2426::pEP105[2]::pNH401[2]	Same as NH2426 except *trp1::hisG::GAL4-ER::TRP1 ura3::ndt80-6D::URA3* *trp1::hisG::GAL4-ER::TRP1 ura3::ndt80-6D::URA3*	This work
NH2426::pEP105[2]::pXC11[2]	Same as NH2426 except *trp1::hisG::GAL4-ER::TRP1 ura3::P_{GAL1}-ndt80-6A::URA3* *trp1::hisG::GAL4-ER::TRP1 ura3::P_{GAL1}-ndt80-6A::URA3*	This work

NH2426::pEP105[2]::pXC12[2]	Same as NH2426 except *trp1::hisG::GAL4-ER::TRP1 ura3::P_{GAL1}-ndt80-6D::URA3* *trp1::hisG::GAL4-ER::TRP1 ura3::P_{GAL1}-ndt80-6D::URA3*	This work
SKY370 ndt80	MAT**a** *ho::LYS2 lys2 ura3 leu2::hisG trp1::hisG arg4-Bgl his4B::LEU2 ndt80::hphMX4*	Nancy Hollingsworth
SKY370 ndt80::pEP105	same as SKY370 ndt80 except *trp1::hisG::GAL4-ER::TRP1*	This work
SKY370 ndt80::pEP105::pBG4	*same as SKY370 ndt80 except trp1::hisG::GAL4-ER::TRP1* *ura3::P_{GAL1}-NDT80::URA3*	This work
SKY370 ndt80::pEP105::pHL8	*same as SKY370 ndt80 except trp1::hisG::GAL4-ER::TRP1* *ura3::NDT80::URA3*	This work
SKY370 ndt80::pEP105::pHL8-R177A	*same as SKY370 ndt80 except trp1::hisG::GAL4-ER::TRP1* *ura3::ndt80-R177A::URA3*	This work
SKY370 ndt80::pEP105::pNH400	*same as SKY370 ndt80 except trp1::hisG::GAL4-ER::TRP1* *ura3::ndt80-6A::URA3*	This work
SKY370 ndt80::pEP105::pNH401	*same as SKY370 ndt80 except trp1::hisG::GAL4-ER::TRP1* *ura3::ndt80-6D::URA3*	This work
SKY370 ndt80::pEP105::pXC11	*same as SKY370 ndt80 except trp1::hisG::GAL4-ER::TRP1* *ura3::P_{GAL1}-ndt80-6A::URA3*	This work

SKY370 ndt80::pEP105::pXC12	*same as SKY370 ndt80 except trp1::hisG::GAL4-ER::TRP1 ura3::P_{GAL1}-ndt80-6D::URA3*	This work
SKY371 ndt80	*MATα leu2::hisG his4X::LEU2 ho::LYS2 lys2 ura3 arg4-nsp trp1::hisG ndt80::hphMX4*	Nancy Hollingsworth
SKY371 ndt80::pEP105	same as SKY371 ndt80 except *trp1::hisG::GAL4-ER::TRP1*	This work
SKY371 ndt80::pEP105::pBG4	same as SKY371 ndt80 except *trp1::hisG::GAL4-ER::TRP1 ura3::P_{GAL1}-NDT80::URA3*	This work
SKY371 ndt80::pEP105::pHL8	same as SKY371 ndt80 except *trp1::hisG::GAL4-ER::TRP1 ura3::NDT80::URA3*	This work
SKY371 ndt80::pEP105::pHL8-R177A	same as SKY371 ndt80 except *trp1::hisG::GAL4-ER::TRP1 ura3::ndt80-R177A::URA3*	This work
SKY371 ndt80::pEP105::pNH400	same as SKY371 ndt80 except *trp1::hisG::GAL4-ER::TRP1 ura3::ndt80-6A::URA3*	This work
SKY371 ndt80::pEP105::pNH401	same as SKY371 ndt80 except *trp1::hisG::GAL4-ER::TRP1 ura3::ndt80-6D::URA3*	This work
SKY371 ndt80::pEP105::pXC11	same as SKY371 ndt80 except *trp1::hisG::GAL4-ER::TRP1 ura3::P_{GAL1}-ndt80-6A::URA3*	This work

SKY371 ndt80::pEP105::pXC12	same as SKY371 ndt80 except *trp1::hisG::GAL4-ER::TRP1* *ura3::P_{GAL1}-ndt80-6D::URA3*	This work

Table 4-2. Plasmids

Name	Yeast Genotype	Source
p4339	*natMX4*	(Tong and Boone, 2005)
pBG1	*URA3 NDT80*	this work
pBG3	*URA3 ndt80-3xGFP*	this work
pBG4	*URA3* P_{GAL1}*-NDT80*	this work
pBG5	*URA3* P_{GAL1}*-ndt80-3xGFP*	this work
pBG9	*LEU2 GFP1-10*	this work
pBG10	*URA3* P_{GAL1}*-NDT80-5xβ11*	this work
pRS305	*LEU2*	(Sikorski and Hieter, 1989)
pRS306	*URA3*	(Sikorski and Hieter, 1989)
pRS425-TEF1-GFP1-10-IDT	*LEU2* P_{TEF1}*-GFP 1-10-*T_{CYC1} *2μ ori*	Yuping Chen
pRS426-GAL1-sc5xGFP11	*URA3 2μ* P_{GAL1}*-5xGFPβ11*	Yuping Chen
pEP102	*TRP1*	(Prugar et al., 2017)
pEP105	*pGPD-GAL4.ER TRP1*	(Prugar et al., 2017)
pFA6a-kanMX6-3xGFP	*kanMX6 3xGFP*	Gang Zhao
pFA6a-kanMX6-PGAL1-GFP	*kanMX6* P_{GAL1}	(Longtine et al., 1998)
pHL8	*URA3 NDT80*	(Lo et al., 2012)
pHL8-R177A	*URA3 NDT80-R177A*	(Lo et al., 2012)
pNH310	*HTB1-mOrange TRP1*	Nancy Hollingsworth
pNH400	*URA3 NDT80- S24A, S205A, T211A, S327A, S329A, S343A*	Nancy Hollingsworth

	(*NDT80-6A*)	
pNH401	*URA3 NDT80- S24D, S205D, T211D, S327D, S329D, S343D* (*NDT80-6D*)	Nancy Hollingsworth
pXC11	*URA3* P_{GAL1}*-NDT80- S24A, S205A, T211A, S327A, S329A, S343A* (P_{GAL1}*-NDT80-6A*)	Xiangyu Chen
pXC12	*URA3* P_{GAL1}*-NDT80- S24D, S205D, T211D, S327D, S329D, S343D* (P_{GAL1}*-NDT80-6D*)	Xiangyu Chen

Table 4-3. Oligonucleotides

Name	Purpose	Sequence
ER-HBD-IN-REV	Confirm insertion of *GAL4-ER*	5’ TTTGAGGCACACAAACTCCT 3’
GAL1-IN-BG	Confirm insertion of P_{GAL1}	5’ TCCTGAAACGCAGATGTG 3’
GAL1-TEST	Confirm insertion of P_{GAL1}	5’ GCCTCGCGCCGCACTGCTCCG AAC 3’
GAL4-SEQ7	Confirm insertion of *GAL4-ER*	5’ AACAGTAGCAACGGTCCG 3’
GFP-NDT80-F1	Forward primer to amplify 5’ end of 3xGFP with a 5’ homology to the 3’ end of *NDT80*	5’ TGAGGAAGATAGTTTCTATAAGT ATATGTCGAAGGGTGAAGAGC 3’
3xGFP-R1	Reverse primer to amplify 3’ end of *3xGFP* with a 3’ homology to the 5’ end of the *NDT80* 3’UTR	5’ TTATTTATACAACTCGTCC 3’
3xGFP-SEQ1-F	Confirm insertion of *3xGFP*	5’ ATGGTAACATACTTGGAC 3’
3xGFP-SEQ2-F	Confirm insertion of *3xGFP*	5’ ATGCCTGAGGGATATGTC 3’
3xGFP-SEQ3-F	Confirm insertion of *3xGFP*	5’ TGCACCACCGGTAAGTTG 3’
3xGFP-SEQ4-R	Confirm insertion of *3xGFP*	5’ CTTTGCTTAATACACTTTGC 3’
GFP1-10-IN	Confirm insertion of *5xGFP1-10*	5’ CGACATTGTGTCTGACGGTG 3’
GFP1-10-OUT	Confirm insertion of *5xGFP1-10*	5’ CTCTTCCAGATTTTCTCGG 3’

5xGFP11-NDT80-UTR-F1	Forward primer to amplify *NDT80* 3' UTR with a 5' homology to the 3' end of *5xGFP11*	5' GTACGTTAACGCCGCGGGTATCACC TAAATAAACTAATGATTTTAAATC 3'
5xGFP11-R1	Reverse primer to amplify 3' end of *5xGFP11* for Gibson Assembly	5' GGTGATACCCGCGGCGTTAAC 3'
NDT80-5xGFP11-F1	Forward primer to amplify *5xGFP11* fragment with 5' homology to the 3' end of *NDT80* orf	5' TGAGGAAGATAGTTTCTATAAGTATGGATCAGGAGCGACAGCATC 3'
NDT80-IN	Confirm insertion of *NDT80* orf	5' CCCACTCTTCATCAATATGGTCG 3'
NDT80-orf-GAL1-F1	Forward primer to amplify *NDT80* ORF with 5' homology to the 3' end of *GAL1* promoter	5' ACCTCTATACTTTAACGTCAAGGAGCTTAAAATGAATGAAATGG 3'
Ndt80-R1	Reverse primer to amplify 3' end of *NDT80* orf for Gibson Assembly	5' ATACTTATAGAAACTATCTTC 3'
NDT80-SEQ1-F	Sequencing primer for *NDT80*	5' ACAGATCCAGTATTACAG 3'
NDT80-SEQ2-F	Sequencing primer for *NDT80*	5' AGAAGCTTCAAATGTTCG 3'
NDT80-SEQ3-F	Sequencing primer for *NDT80*	5' TGAGAACACCGTCGAGTG 3'
NDT80-SEQ4-F	Sequencing primer for *NDT80*	5' AGCTATGGTAACGAACTC 3'
NDT80-SEQ5-R	Sequencing primer for *NDT80*	5' TCTCACTAATTCAAATGG 3'

NDT80-SEQ6-F	Sequencing primer for *NDT80*	5’ ACCTCCAGATAACTTGACC 3’
NDT80-SEQ7-R	Sequencing primer for *NDT80*	5’ TGAAAAGTGAGACCAATC 3’
NDT80-UTR-GFP-F1	Forward primer to amplify *NDT80* 3’ UTR with 5’ homology to the 3’ end of *3xGFP* sequence	5’ CGGTATGGACGAGTTGTATAAATAAATAAACTAATGATTTTAAATCG 3’
NDT80-WT-EcoRI-F1	Forward primer to amplify *NDT80* upstream promoter region with a 5’ homology to the EcoRI cut site of pRS306 for Gibson Assembly	5’ TGGATCCCCCGGGCTGCAGGAATTCTAAATAACGGTTTTTACAATGG 3’
NDT80-WT-ClaI-R1	Reverse primer to amplify *NDT80* 3’ UTR with 3’ homology to the ClaI cut site of pRS306 for Gibson Assembly	5’ CCCCCTCGAGGTCGACGGTATCGATTCCCTTTTGTGAACTTCAAG 3’
pGAL1-EcoRI-F1	Forward primer to amplify P_{GAL1} promoter with a 5’ homology to the EcoRI cut site of pRS306 for Gibson Assembly	5’ ACTAGTGGATCCCCCGGGCTGCAGGCGGATTAGAAGCCGCCGAG 3’
pGAL1-R1	Reverse primer to amplify *GAL1* promoter for Gibson Assembly	5’ CTCCTTGACGTTAAAGTATAG 3’
TEST-NDT80	Confirm insertion of *NDT80* upstream promoter region	5’ GACGTTTTCTGCTTCAGGTGCG 3’
TRP1-5-nat-F1	Forward primer to amplify *natMX4* gene with homologous ends to 5’ end of *TRP1* for knockout	5’ TATTGAGCACGTGAGTATACGTGATTAAGCACACAAAGGCAGCTTGGAGTACATGGAGGCCCAGAATACCC 3’

TRP1-5-nat-R1	Reverse primer to amplify *natMX4* gene with homologous ends to 5' end of *TRP1* for knockout	5' TCATTGACCAGAGCCAAAACAT CCTCCTTAGGTTGATTACGAAA CACGCCCAGTATAGCGACCAGC ATTCAC 3'

Table 4-4. Antibodies

Protein	Arp7	Cdc5	Clb1	Ndt80
Primary Antibody	Goat α-Arp7	Goat α-Cdc5	Goat α-Clb1	Rabbit α-Ndt80
Dilution	1:50000	1:500	1:300	1:15000
Incubation	4°C ON	4°C ON	4°C ON	RT 2h
Source	Santa Cruz sc-8961	Santa Cruz sc-6733	Santa Cruz sc-7647	Michael Lichten
Secondary Antibody	Mouse α-goat	Mouse α-goat	Mouse α-goat	Goat α-rabbit
Dilution	1:15000	1:15000	1:10000	1:10000
Incubation	RT 1h	RT 1h	RT 1h	RT 1h
Source	Santa Cruz sc-2354	Santa Cruz sc-2354	Santa Cruz sc-2354	Santa Cruz sc-2004

References

Ahmed, N.T., Bungard, D., Shin, M.E., Moore, M., and Winter, E. (2009). The Ime2 protein kinase enhances the disassociation of the Sum1 repressor from middle meiotic promoters. Mol Cell Biol *29*, 4352-4362.

Benjamin, K.R., Zhang, C., Shokat, K.M., and Herskowitz, I. (2003). Control of landmark events in meiosis by the CDK Cdc28 and the meiosis-specific kinase Ime2. Genes Dev *17*, 1524-1539.

Bergerat, A., de Massy, B., Gadelle, D., Varoutas, P.C., Nicolas, A., and Forterre, P. (1997). An atypical topoisomerase II from Archaea with implications for meiotic recombination. Nature *386*, 414-417.

Bishop, D.K. (1994). RecA homologs Dmc1 and Rad51 interact to form multiple nuclear complexes prior to meiotic chromosome synapsis. Cell *79*, 1081-1092.

Bishop, D.K., Park, D., Xu, L., and Kleckner, N. (1992). DMC1: a meiosis-specific yeast homolog of *E. coli* recA required for recombination, synaptonemal complex formation, and cell cycle progression. Cell *69*, 439-456.

Boeke, J.D., Trueheart, J., Natsoulis, G., and Fink, G.R. (1987). 5-Fluoroorotic acid as a selective agent in yeast molecular genetics. Methods Enzymol *154*, 164-175.

Börner, G.V., Kleckner, N., and Hunter, N. (2004). Crossover/noncrossover differentiation, synaptonemal complex formation, and regulatory surveillance at the leptotene/zygotene transition of meiosis. Cell *117*, 29-45.

Brown, M.S., Grubb, J., Zhang, A., Rust, M.J., and Bishop, D.K. (2015). Small Rad51 and Dmc1 complexes often co-occupy both ends of a meiotic DNA double strand break. PLoS Genet *11*, e1005653.

Callender, T.L., Laureau, R., Wan, L., Chen, X., Sandhu, R., Laljee, S., Zhou, S., Suhandynata, R.T., Prugar, E., Gaines, W.A.*, et al.* (2016). Mek1 down regulates Rad51 activity during yeast meiosis by phosphorylation of Hed1. PLoS Genet *12*, e1006226.

Cao, L., Alani, E., and Kleckner, N. (1990). A pathway for generation and processing of double-strand breaks during meiotic recombination in *S. cerevisiae*. Cell *61*, 1089-1101.

Carballo, J.A., Johnson, A.L., Sedgwick, S.G., and Cha, R.S. (2008). Phosphorylation of the axial element protein Hop1 by Mec1/Tel1 ensures meiotic interhomolog recombination. Cell *132*, 758-770.

Carlile, T.M., and Amon, A. (2008). Meiosis I is established through division-specific translational control of a cyclin. Cell *133*, 280-291.

Chen, X., Suhandynata, R.T., Sandhu, R., Rockmill, B., Mohibullah, N., Niu, H., Liang, J., Lo, H.C., Miller, D.E., Zhou, H.*, et al.* (2015). Phosphorylation of the synaptonemal complex protein Zip1 regulates the crossover/noncrossover decision during yeast meiosis. PLoS Biol *13*, e1002329.

Chu, S., DeRisi, J., Eisen, M., Mulholland, J., Botstein, D., Brown, P.O., and Herskowitz, I. (1998). The transcriptional program of sporulation in budding yeast. Science *282*, 699-705.

Chu, S., and Herskowitz, I. (1998). Gametogenesis in yeast is regulated by a transcriptional cascade dependent on Ndt80. Mol Cell *1*, 685-696.

Cloud, V., Chan, Y.L., Grubb, J., Budke, B., and Bishop, D.K. (2012). Rad51 is an accessory factor for Dmc1-mediated joint molecule formation during meiosis. Science *337*, 1222-1225.

Curran, K.A., Karim, A.S., Gupta, A., and Alper, H.S. (2013). Use of expression-enhancing terminators in *Saccharomyces cerevisiae* to increase mRNA half-life and improve gene expression control for metabolic engineering applications. Metab Eng *19*, 88-97.

Dahmann, C., and Futcher, B. (1995). Specialization of B-type cyclins for mitosis or meiosis in *S. cerevisiae*. Genetics *140*, 957-963.

de los Santos, T., Loidl, J., Larkin, B., and Hollingsworth, N.M. (2001). A role for *MMS4* in the processing of recombination intermediates during meiosis in *Saccharomyces cerevisiae*. Genetics *159*, 1511-1525.

Dong, H., and Roeder, G.S. (2000). Organization of the yeast Zip1 protein within the central region of the synaptonemal complex. J Cell Biol *148*, 417-426.

Dresser, M.E., Ewing, D.J., Conrad, M.N., Dominguez, A.M., Barstead, R., Jiang, H., and Kodadek, T. (1997). *DMC1* functions in a *Saccharomyces cerevisiae* meiotic pathway that is largely independent of the *RAD51* pathway. Genetics *147*, 533-544.

Ephrussi, B., and Slonimski, P.P. (1955). Subcellular units involved in the synthesis of respiratory enzymes in yeast. Nature *176*, 1207-1208.

Falk, J.E., Chan, A.C., Hoffmann, E., and Hochwagen, A. (2010). A Mec1- and PP4-dependent checkpoint couples centromere pairing to meiotic recombination. Dev Cell *19*, 599-611.

Hassold, T., and Hunt, P. (2001). To err (meiotically) is human: the genesis of human aneuploidy. Nat Rev Genet *2*, 280-291.

Hepworth, S.R., Ebisuzaki, L.K., and Segall, J. (1995). A 15-base-pair element activates the *SPS4* gene midway through sporulation in *Saccharomyces cerevisiae*. Mol Cell Biol *15*, 3934-3944.

Hepworth, S.R., Friesen, H., and Segall, J. (1998). *NDT80* and the meiotic recombination checkpoint regulate expression of middle sporulation-specific genes in *Saccharomyces cerevisiae*. Molecular and Cellular Biology *18*, 5750-5761.

Hollingsworth, N.M., Goetsch, L., and Byers, B. (1990). The *HOP1* gene encodes a meiosis-specific component of yeast chromosomes. Cell *61*, 73-84.

Hong, E.L., Shinohara, A., and Bishop, D.K. (2001). *Saccharomyces cerevisiae* Dmc1 protein promotes renaturation of single-strand DNA (ssDNA) and assimilation of ssDNA into homologous super-coiled duplex DNA. J Biol Chem *276*, 41906-41912.

Johnston, M. (1987). A model fungal gene regulatory mechanism: the *GAL* genes of *Saccharomyces cerevisiae*. Microbiol Rev *51*, 458-476.

Kamiyama, D., Sekine, S., Barsi-Rhyne, B., Hu, J., Chen, B., Gilbert, L.A., Ishikawa, H., Leonetti, M.D., Marshall, W.F., Weissman, J.S.*, et al.* (2016). Versatile protein tagging in cells with split fluorescent protein. Nat Commun *7*, 11046.

Keeney, S., Giroux, C.N., and Kleckner, N. (1997). Meiosis-specific DNA double-strand breaks are catalyzed by Spo11, a member of a widely conserved protein family. Cell *88*, 375-384.

Klein, F., Mahr, P., Galova, M., Buonomo, S.B., Michaelis, C., Nairz, K., and Nasmyth, K. (1999). A central role for cohesins in sister chromatid cohesion, formation of axial elements, and recombination during yeast meiosis. Cell *98*, 91-103.

Kohl, K.P., and Sekelsky, J. (2013). Meiotic and mitotic recombination in meiosis. Genetics *194*, 327-334.

Lamoureux, J.S., and Glover, J.N. (2006). Principles of protein-DNA recognition revealed in the structural analysis of Ndt80-MSE DNA complexes. Structure *14*, 555-565.

Lamoureux, J.S., Stuart, D., Tsang, R., Wu, C., and Glover, J.N. (2002). Structure of the sporulation-specific transcription factor Ndt80 bound to DNA. EMBO J *21*, 5721-5732.

Liu, Y., Gaines, W.A., Callender, T., Busygina, V., Oke, A., Sung, P., Fung, J.C., and Hollingsworth, N.M. (2014). Down-regulation of Rad51 activity during meiosis in yeast prevents competition with Dmc1 for repair of double-strand breaks. PLoS Genet *10*, e1004005.

Lo, H.C., and Hollingsworth, N.M. (2011). Using the semi-synthetic epitope system to identify direct substrates of the meiosis-specific budding yeast kinase, Mek1. Methods Mol Biol *745*, 135-149.

Lo, H.C., Kunz, R.C., Chen, X., Marullo, A., Gygi, S.P., and Hollingsworth, N.M. (2012). Cdc7-Dbf4 is a gene-specific regulator of meiotic transcription in yeast. Mol Cell Biol *32*, 541-557.

Loidl, J. (2016). Conservation and variability of meiosis across the eukaryotes. Annu Rev Genet *50*, 293-316.

Longtine, M.S., McKenzie, A., 3rd, Demarini, D.J., Shah, N.G., Wach, A., Brachat, A., Philippsen, P., and Pringle, J.R. (1998). Additional modules for versatile and economical PCR-based gene deletion and modification in *Saccharomyces cerevisiae*. Yeast *14*, 953-961.

Lydall, D., Nikolsky, Y., Bishop, D.K., and Weinert, T. (1996). A meiotic recombination checkpoint controlled by mitotic checkpoint genes. Nature *383*, 840-843.

Lynn, A., Soucek, R., and Börner, G.V. (2007). ZMM proteins during meiosis: crossover artists at work. Chromosome Res *15*, 591-605.

Mok, J., Kim, P.M., Lam, H.Y., Piccirillo, S., Zhou, X., Jeschke, G.R., Sheridan, D.L., Parker, S.A., Desai, V., Jwa, M.*, et al.* (2010). Deciphering protein kinase specificity through large-scale analysis of yeast phosphorylation site motifs. Sci Signal *3*, ra12.

Montano, S.P., Cote, M.L., Fingerman, I., Pierce, M., Vershon, A.K., and Georgiadis, M.M. (2002). Crystal structure of the DNA-binding domain from Ndt80, a transcriptional activator required for meiosis in yeast. Proc Natl Acad Sci U S A *99*, 14041-14046.

Niu, H., Li, X., Job, E., Park, C., Moazed, D., Gygi, S.P., and Hollingsworth, N.M. (2007). Mek1 kinase is regulated to suppress double-strand break repair between sister chromatids during budding yeast meiosis. Mol Cell Biol *27*, 5456-5467.

Niu, H., Wan, L., Baumgartner, B., Schaefer, D., Loidl, J., and Hollingsworth, N.M. (2005). Partner choice during meiosis is regulated by Hop1-promoted dimerization of Mek1. Mol Biol Cell *16*, 5804-5818.

Niu, H., Wan, L., Busygina, V., Kwon, Y., Allen, J.A., Li, X., Kunz, R.C., Kubota, K., Wang, B., Sung, P.*, et al.* (2009). Regulation of meiotic recombination via Mek1-mediated Rad54 phosphorylation. Mol Cell *36*, 393-404.

Orr-Weaver, T.L., Szostak, J.W., and Rothstein, R.J. (1981). Yeast transformation: a model system for the study of recombination. Proc Natl Acad Sci U S A *78*, 6354-6358.

Ozsarac, N., Straffon, M.J., Dalton, H.E., and Dawes, I.W. (1997). Regulation of gene expression during meiosis in *Saccharomyces cerevisiae*: *SPR3* is controlled by both ABFI and a new sporulation control element. Mol Cell Biol *17*, 1152-1159.

Padmore, R., Cao, L., and Kleckner, N. (1991). Temporal comparison of recombination and synaptonemal complex formation during meiosis in *S. cerevisiae*. Cell *66*, 1239-1256.

Pak, J., and Segall, J. (2002). Regulation of the premiddle and middle phases of expression of the *NDT80* gene during sporulation of *Saccharomyces cerevisiae*. Mol Cell Biol *22*, 6417-6429.

Partow, S., Siewers, V., Bjorn, S., Nielsen, J., and Maury, J. (2010). Characterization of different promoters for designing a new expression vector in *Saccharomyces cerevisiae*. Yeast *27*, 955-964.

Prugar, E., Burnett, C., Chen, X., and Hollingsworth, N.M. (2017). Coordination of double strand break repair and meiotic progression in yeast by a Mek1-Ndt80 negative feedback loop. Genetics *206*, 497-512.

Rockmill, B., and Roeder, G.S. (1991). A meiosis-specific protein kinase homolog required for chromosome synapsis and recombination. Genes Dev *5*, 2392-2404.

Rothstein, R. (1991). Targeting, disruption, replacement, and allele rescue: integrative DNA transformation in yeast. Methods Enzymol *194*, 281-301.

Shin, M.E., Skokotas, A., and Winter, E. (2010). The Cdk1 and Ime2 protein kinases trigger exit from meiotic prophase in *Saccharomyces cerevisiae* by inhibiting the Sum1 transcriptional repressor. Mol Cell Biol *30*, 2996-3003.

Sikorski, R.S., and Hieter, P. (1989). A system of shuttle vectors and yeast host strains designed for efficient manipulation of DNA in *Saccharomyces cerevisiae*. Genetics *122*, 19-27.

Smith, A.V., and Roeder, G.S. (1997). The yeast Red1 protein localizes to the cores of meiotic chromosomes. J Cell Biol *136*, 957-967.

Sopko, R., Raithatha, S., and Stuart, D. (2002). Phosphorylation and maximal activity of *Saccharomyces cerevisiae* meiosis-specific transcription factor Ndt80 is dependent on Ime2. Mol Cell Biol *22*, 7024-7040.

Sourirajan, A., and Lichten, M. (2008). Polo-like kinase Cdc5 drives exit from pachytene during budding yeast meiosis. Genes Dev *22*, 2627-2632.

Storlazzi, A., Xu, L., Schwacha, A., and Kleckner, N. (1996). Synaptonemal complex (SC) component Zip1 plays a role in meiotic recombination independent of SC polymerization along the chromosomes. Proc Natl Acad Sci U S A *93*, 9043-9048.

Suhandynata, R.T., Wan, L., Zhou, H., and Hollingsworth, N.M. (2016). Identification of putative Mek1 substrates during meiosis in *Saccharomyces cerevisiae* using quantitative phosphoproteomics. PLoS One *11*, e0155931.

Sun, H., Treco, D., Schultes, N.P., and Szostak, J.W. (1989). Double-strand breaks at an initiation site for meiotic gene conversion. Nature *338*, 87-90.

Sun, H., Treco, D., and Szostak, J.W. (1991). Extensive 3'-overhanging, single-stranded DNA associated with the meiosis-specific double-strand breaks at the *ARG4* recombination initiation site. Cell *64*, 1155-1161.

Sym, M., Engebrecht, J.A., and Roeder, G.S. (1993). ZIP1 is a synaptonemal complex protein required for meiotic chromosome synapsis. Cell *72*, 365-378.

Tong, A.H.Y.T., and Boone, C. (2005). Synthetic Genetic Array (SGA) analysis in *Saccharomyces cerevisiae*. Methods in Molecular Biology *313*, 171-192.

Tung, K.S., Hong, E.J., and Roeder, G.S. (2000). The pachytene checkpoint prevents accumulation and phosphorylation of the meiosis-specific transcription factor Ndt80. Proc Natl Acad Sci U S A *97*, 12187-12192.

Tung, K.S., and Roeder, G.S. (1998). Meiotic chromosome morphology and behavior in *zip1* mutants of *Saccharomyces cerevisiae*. Genetics *149*, 817-832.

Wan, L., de los Santos, T., Zhang, C., Shokat, K., and Hollingsworth, N.M. (2004). Mek1 kinase activity functions downstream of *RED1* in the regulation of meiotic double strand break repair in budding yeast. Mol Biol Cell *15*, 11-23.

Wang, Y., Chang, C.Y., Wu, J.F., and Tung, K.S. (2011). Nuclear localization of the meiosis-specific transcription factor Ndt80 is regulated by the pachytene checkpoint. Mol Biol Cell *22*, 1878-1886.

Winter, E. (2012). The Sum1/Ndt80 transcriptional switch and commitment to meiosis in *Saccharomyces cerevisiae*. Microbiol Mol Biol Rev *76*, 1-15.

Xu, L., Ajimura, M., Padmore, R., Klein, C., and Kleckner, N. (1995). *NDT80*, a meiosis-specific gene required for exit from pachytene in *Saccharomyces cerevisiae*. Mol Cell Biol *15*, 6572-6581.

Xu, L., Weiner, B.M., and Kleckner, N. (1997). Meiotic cells monitor the status of the interhomolog recombination complex. Genes Dev *11*, 106-118.